ADVANCED ENGINEERING MATERIALS
www.aem-journal.com

Nanoengineering of Metallic Glasses

*Jianan Fu and Jiang Ma**

Metallic glasses with nanostructures recently have attracted extensive attention in various fields due to their unique functional properties. The amorphous atomic structure and nanoscale forms are the fundamental features of these nanomaterials. Herein, the current nanoengineering approaches for fabricating the metallic glasses with nanostructures such as thermoplastic forming, ultrasonic plasticity forming, dealloying, etc., are systematically summarized and the morphology and composition of the various types of metallic glasses with nanostructures that are formed by nanoengineering are classified. In addition, the functional properties and applications of metallic glasses with nanostructures are focused on. On the basis of this comprehensive review, some options for optimizing nanoengineering and anticipating the potential functional applications of metallic glasses with nanostructures are proposed.

1. Introduction

Different from the previous approaches of discovering new functional materials by regulating the element compositions, in principle, the properties of materials significantly change at nanoscale or smaller structural dimensions,[1–4] giving rise to inspirations for designing new materials with superior properties. As a novel functional material, nanomaterials, since their discovery,[1] have led to a boom in research into diverse fields due to their unique properties, such as water treatment,[5–8] photothermal therapy,[9–12] catalysis,[13–16] wettability,[17–20] light absorbers,[21–24] triboelectric nanogenerators,[25–28] detectors,[29–32] nanoagriculture,[33–36] etc. Additive and subtractive manufacturing approaches are currently two most prominent processes for designing nanomaterials[37–40] and have been used extensively to fabricate nanostructures of various materials such as polymers,[41,42] monolithic metals,[43,44] glass,[45,46] amorphous alloys,[47,48] crystalline alloys,[49,50] etc. Driven by this boom, nanomaterials are also becoming mainstream in all fields of materials.

In recent years, amorphous alloys have also begun to be introduced into research in the field of nanomaterials. Amorphous alloys, also known as metallic glasses (MGs), were first discovered in 1960s.[51] MGs obtained at rapid cooling rates exhibit a short-range-ordered and long-range-disordered atomic structure,[52–55] which endow them with superior properties compared with crystalline alloys, such as thermoplasticity,[56,57] ultrasonic plasticity,[58,59] high strength and toughness,[60,61] corrosion and wear resistance,[62,63] catalytic properties,[64,65] etc.[66–68] However, this unique atomic structure also makes MGs have lack of plastic deformation caused by grains and grain boundaries inherent in crystalline alloys, and it is difficult to process MGs at room temperature by conventional processing methods, which greatly increases the challenge of fabricating MGs with nanostructures. The development of engineering technologies for MGs, in particular nanoengineering, is expected to promote MGs in functional applications.

Following continuous exploration, a variety of engineering methods for fabricating MGs with nanostructures have emerged, and these MGs with nanostructures fabricated by nanoengineering approaches have shown some excellent properties. As shown in **Figure 1**, this paper focuses on a review of recent nanoengineering methods for the formation of MGs with nanostructures including thermoplastic forming (TPF), ultrasonic plasticity forming (UPF), dealloying, sputtering, laser processing, etc. In addition, some existing or potential functional applications of these MGs with nanostructures are systematically reviewed such as hydrophobic, catalysis, cellular response, drug injection, desalination, etc. Based on these reviews, the paper not only discusses potential optimized schemes that can be used to fabricate MGs with nanostructures, but also concludes with an outlook on the advanced applications of existing MGs with nanostructures in frontier fields.

2. Fabrication Method of MGs with Nanostructures

2.1. TPF

The most widespread and representative nanoengineering for fabricating MGs with nano-structures is TPF,[69–71] which is nanoengineering developed based on the thermoplasticity of MGs itself. As mentioned earlier, MGs have high strength and brittle nature at room temperature, which makes it difficult to process and form. However, when the MGs are in a specific temperature region (i.e., supercooled liquid region [SLR], the range of SLR is determined by the difference between the crystallization temperature (T_x) and the glass transition temperature (T_g) of MGs), this hard and brittle property at room temperature will be transformed into superplasticity.[72,73] In the SLR, the viscosity of MGs will reduce with the temperature rise,[74] so that MGs can be processed and formed like

J. Fu, J. Ma
Shenzhen Key Laboratory of High Performance Nontraditional Manufacturing
College of Mechatronics and Control Engineering
Shenzhen University
Shenzhen 518060, China
E-mail: majiang@szu.edu.cn

The ORCID identification number(s) for the author(s) of this article can be found under https://doi.org/10.1002/adem.202200659.

DOI: 10.1002/adem.202200659

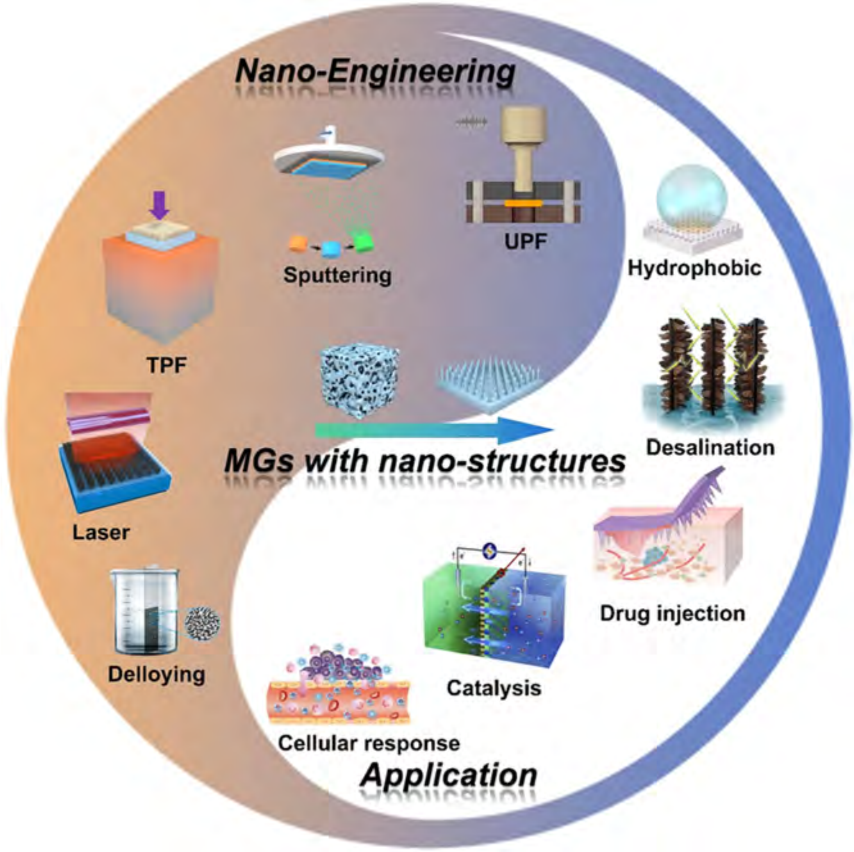

Figure 1. The summary of nanoengineering and the functional applications for MGs with nanostructures. Reproduced with permission.[145] Copyright 2020, Elsevier. Reproduced with permission.[146] Copyright 2020, Nature Publishing Group. Reproduced with permission.[147] Copyright 2022, Elsevier. Reproduced with permission.[148] Copyright 2022, Springer. Reproduced with permission.[149] Copyright 2022, Wiley-VCH. Reproduced with permission.[150] Copyright 2020, Wiley-VCH. Reproduced with permission.[151] Copyright 2021, Elsevier. Reproduced with permission.[152] Copyright 2020, Elsevier. Reproduced with permission.[153] Copyright 2018, Wiley-VCH.

traditional glass or plastic. Furthermore, benefiting from the inherent disordered atomic structure of MGs, the cross-scale structures from micro- to nano- and then to atomic level can be easily realized on the MG surface by the TPF process.[75–77]

As shown in **Figure 2**a, the experimental steps on fabricating MGs with nanostructures by the TPF process can be divided as follows: 1) MGs and nanotemplates are stacked up and down on the heating stage; 2) pressure is applied to the MGs' surfaces after heating it to the SLR; and 3) there is release of the fabricated MGs with nanostructures by removing the nanotemplates.[78] The second step plays an important role in the TPF process for fabricating the MGs with nanostructures. In this step, factors such as temperature, pressure, time during the TPF process, forming size, etc. will influence the forming quality of MGs with nanostructures. Previous works have found that when the MGs are in its SLR, MGs exist in the form of high viscosity.[79] The Hagen–Poiseuille equation can be used to quantitatively describe the influence of various factors on the forming quality during the TPF process.

The corresponding equation is as follows

$$P = \frac{32\eta}{t}\left(\frac{l}{d}\right)^2 \tag{1}$$

In Equation (1), P is the pressure applied to the MGs, t is the duration of the TPF process, l is the length of the structures by the TPF, d represents the diameter of the structures, and η is the viscosity of the MGs.[72,80]

The viscosity is considered to be a key factor influencing the forming quality in Equation (1), and it is worth noting that this equation is only used for forming the MGs with microscale structures.

Recently, some researchers have proposed that viscosity is not only the factors influencing the forming quality during the TPF process. The effect of capillary forces cannot be ignored when the formed structures reach the nanoscale. In this regard, Kumar et al. modified the Hagen–Poiseuille equation to combine viscosity and capillary forces, and the resulting Equation (2) can be used to accurately describe the TPF process when forming MGs with nanostructures.[47]

$$P = \frac{32\eta}{t}\left(\frac{l}{d}\right)^2 - \frac{4\gamma\cos\theta}{d} \tag{2}$$

γ is the vacuum interfacial energy of MGs and θ is the contact angle (CA) between viscous fluid and nanotemplate.[47,72]

Under the extrapolation of Equation (2), the fabrication of platinum (Pt)-based nanowires with different diameters of 13, 35,

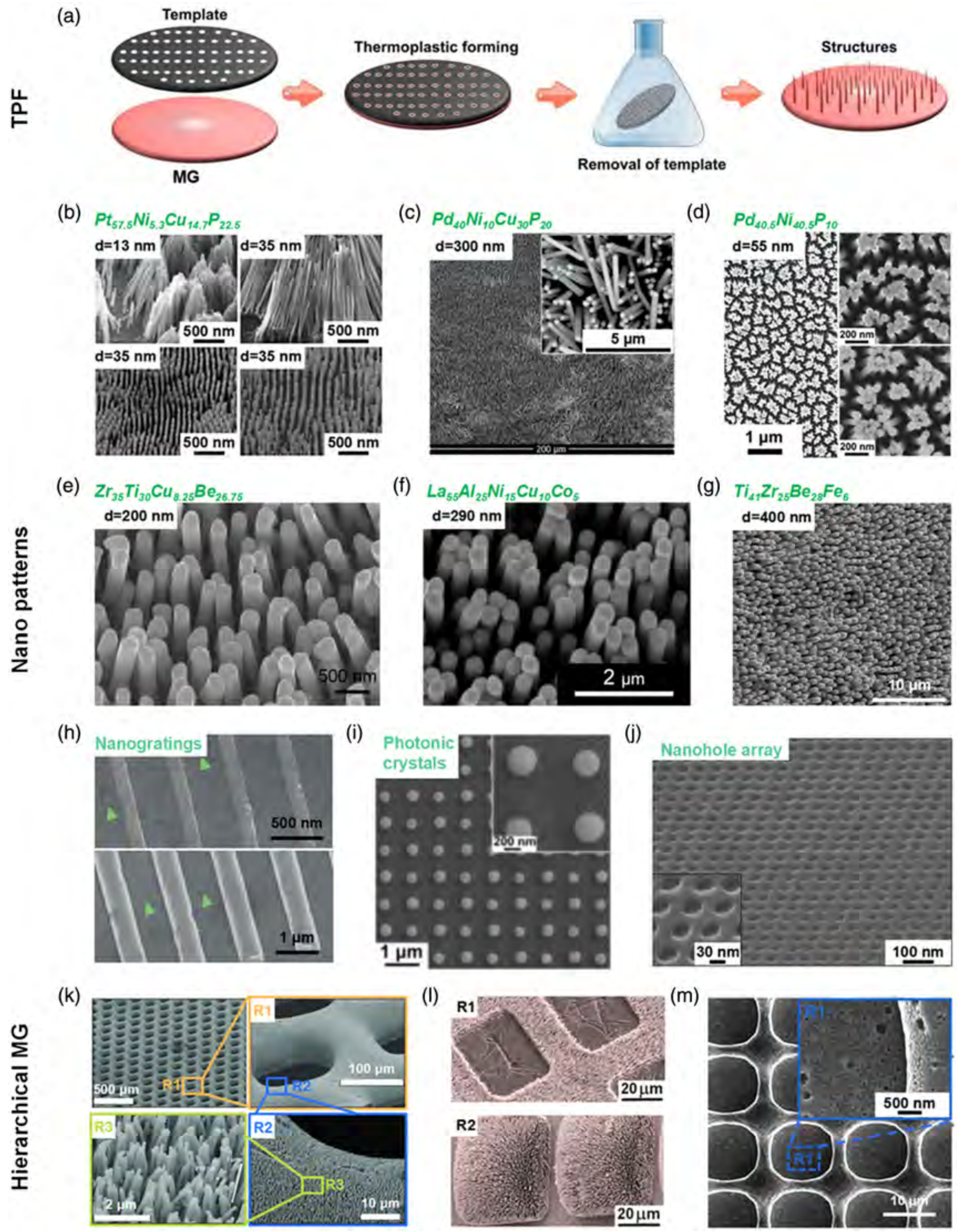

Figure 2. Fabrication of MGs with nanostructures by TPF. a) The schematic diagram for fabricating MGs with nanostructures by TPF process. Reproduced with permission.[78] Copyright 2021, The Royal Society of Chemistry. b) The nanowires of $Pt_{57.5}Cu_{14.7}Ni_{5.3}P_{22.5}$ MG. Reproduced with permission.[47] Copyright 2009, Nature Publishing Group. c) The nanowires of $Pd_{40}Cu_{30}Ni_{10}P_{20}$ MG. Reproduced with permission.[78] Copyright 2021, The Royal Society of Chemistry. d) The nanowires of $Pd_{40.5}Ni_{40.5}P_{19}$ MG. Reproduced with permission.[81] Copyright 2014, Elsevier. e) The nanowires of $Zr_{35}Ti_{30}Cu_{8.25}Be_{26.75}$ MG. Reproduced with permission.[82] Copyright 2015, IOP Publishing. f) The nanowires of $La_{55}Al_{25}Ni_{15}Cu_{10}Co_5$ MG. Reproduced with permission.[83] Copyright 2021, Elsevier. g) The nanowires of $Ti_{41}Zr_{25}Be_{28}Fe_6$ MG. Reproduced with permission.[84] Copyright 2018, Elsevier. h) The nanogratings on MG. Reproduced with permission.[85] Copyright 2007, AIP. i) The photonic crystals on MG. Reproduced with permission.[86] Copyright 2015, Elsevier. j) The nanoholes on MG. Reproduced with permission.[87] Copyright 2010, Elsevier. k) The hierarchical structure of $Pt_{57.5}Cu_{14.7}Ni_{5.3}P_{22.5}$ MG. Reproduced with permission.[88] Copyright 2013, Wiley-VCH. Copyright 2010, Elsevier. l) The hierarchical structure of $Pt_{57.5}Cu_{14.7}Ni_{5.3}P_{22.5}$ MG. Reproduced with permission.[89] Copyright 2015, American Chemical Society. m) The hierarchical structure of $Pt_{57.5}Cu_{14.7}Ni_{5.3}P_{22.5}$ MG. Reproduced with permission.[90] Copyright 2014, AIP.

55 nm and the aspect ratio over 50 was achieved by controlling the experimental parameters during the TPF process (see Figure 2b).[47] The publication of work has also led many researchers to invest in the field of TPF. After that, MGs with different compositions have also been used for this process. Ma et al. successfully fabricated nanowires with a diameter of 300 nm on the $Pd_{40}Ni_{10}Cu_{30}P_{20}$ MG surface by the TPF process (see Figure 2c) and utilized it as carrier for the deposition of Pt nanoparticles. $Pd_{40.5}Ni_{40.5}P_{19}$ in palladium (Pd)-based MG systems also realizes the formation of nanowires with a diameter of 55 nm (see Figure 2d).[81] Noble metal-based MGs system are often selected for the TPF process due to its excellent oxidation resistance. However, in addition to the noble metal-based MGs, some non-noble metal-based MGs systems have also been developed for TPF. Liu et al. fabricated nanowires with a diameter of ≈200 nm on the $Zr_{35}Ti_{30}Cu_{8.25}Be_{26.75}$ MG by adding an oil layer to wet the nanotemplates (see Figure 2e).[82] Ma et al. achieved the formation of nanowires with diameters of ≈330, 290, and 170 nm on the $La_{55}Al_{25}Ni_{5}Cu_{10}Co_{5}$ MG surface in a high-vacuum environment (see Figure 2f).[83] Gong et al. explored a $Ti_{41}Zr_{25}Be_{28}Fe_{6}$ MG with excellent TPF ability by optimizing the composition of MGs and fabricated the nanowires with a diameter of ≈400 nm on its surface (see Figure 2g).[84] In addition, the nanostructures on MG surfaces by the TPF process are not only limited to nanowires, but also uniform nanostructures such as nanogratings,[85] photonic crystals,[86] and nanoholes[87] can be formed (see Figure 2h-j). It is difficult to form hierarchical structures on MG surfaces due to the lack of appropriate templates, but some researchers have also successfully fabricated hierarchical structures on MG surfaces by the secondary TPF process. Figure 2k–m shows some hierarchical structures including the formation of nanowires on arrays with uniform micropores and the formation of nanostructures on the uniform microconvex array surface.[88–90] From the aforementioned work on MGs for TPF process, it can be seen that templates are an essential part for fabricating the MGs with nanostructures. The TPF templates currently used for the formation of MGs with nanostructures or atomic-scale structures are broadly the following: anodic aluminum oxide (AAO),[78] silicon (Si) templates,[85] bulk MG (BMG),[47] mica,[91] strontium titanate (STO),[75] lanthanum aluminate ($LaAlO_3$),[92] etc. Among these, Schroers et al. used mica, STO, and $LaAlO_3$ as templates to achieve atomic precision on MGs by TPF process.[75,91,92] In contrast, AAO and Si templates are most commonly used to fabricate MGs with nanostructures by the TPF process. In principle, all kinds of nanostructures can be fabricated on the MG surface by the TPF process if appropriate nanotemplates are available. The TPF process as a nanoengineering approach has given a great impetus to the advancement of MGs into the nanofield and makes MGs no longer limited to the research of structural materials and is expected to expand within the field of nanofunctional applications.

2.2. Dealloying

Dealloying is an advanced nanoengineering technique to fabricate the MGs with nanostructures, and the availability of applying this nanoengineering technique to MGs is largely due to the development of MGs itself. Within the development of MGs, many elements of the periodic table have been used in the composition of MGs, not least some of the more exotic elements such as oxygen (O),[93] hydrogen (H),[94] scandium (Sc),[95] etc. The rich elemental composition provides the preconditions for dealloying to fabricate MGs with nanostructures. The dealloying to form MGs with nanostructures differs markedly from the TPF process in that it involves the selective removal of elements from the MG component to obtain nanostructures.[96,97] Dealloying has the following advantages over the TPF process. 1) No need for templates to be used during the fabrication of nanostructures. 2) The fabricated nanostructures are mostly complex, disordered porous structures, which are not achievable with the TPF process. 3) The size of the nanostructures can also be regulated by the time for selective dissolution.

The principle mechanism in most dealloying methods for the fabrication of MGs with nanostructures is the use of specific chemicals or other electrochemical techniques to remove the less valuable atoms from within the MGs, while retaining the valuable atoms. The schematic in **Figure 3**a clearly demonstrates the process of fabricating MGs with nanostructures by dealloying.[98] Jia et al. fabricated a 3D self-supported nanosponge with a large specific surface area by removing copper (Cu) and nickel (Ni) from $Pd_{20}Pt_{20}Cu_{20}Ni_{20}P_{20}$ high-entropy MGs using a simple one-step dealloying process (see Figure 3b).[98] Besides high-entropy MGs, Doubek et al. similarly removed Ni and Cu from the $Pt_{42.5}Cu_{27}Ni_{9.5}P_{21}$ nanowires fabricated by TPF to form a nanoporous layer on the nanowire surface (see Figure 3c).[99] In addition to single porous nanostructures, the dealloying methods can also achieve the fabrication of hierarchical porous structures. Xu et al. fabricated porous cone-shaped protrusions on the $Au_{55}Cu_{25}Si_{20}$ MG surface by removing the Cu atoms from this MG, and they explained that the formation of the hierarchical structure is related to the atomic-level structure of the initial MG state (see Figure 3d).[100] The recently developed $Ir_{25}Ni_{33}Ta_{42}$ MG[101] with excellent mechanical, corrosion resistance and high-temperature resistance has also been used for fabricating the nanoporous structures. Liu et al. used this MG to successfully fabricate nanoporous structures by dealloying to remove Ni (see Figure 3e).[102] Many non-noble metal-based MG systems are also widely used to fabricate MGs with nanostructures by dealloying. For example, Qian et al. removed aluminum (Al) and titanium (Ti) from $Cu_{45}Al_{45}Ti_{10}$ to fabricate nanopore-constituting face center cubic (fcc) Cu ligaments of 39-79 nm thickness (see Figure 3f).[103] Zhang et al. removed Al and Cu from another Cu-based MG ($Cu_{60}Al_{10}Ce_{25}Pt_{4}Ru_{1}$) to fabricate nanosheets (see Figure 3g),[104] and nanoporous structures were fabricated by removing zirconium (Zr) and Ti from Ni-based MGs by Li et al. (see Figure 3h).[105] It is worth mentioning that Li et al. found that under the same dealloying process, different compositions of Ni-based MGs also affect the morphology of the formed porous structure, and this may provide a potential idea for regulating the morphology of nanostructures.[105] Furthermore, some MGs containing rare-earth elements are also suitable for the formation of MGs with nanostructures by dealloying. Wang et al. added a small amount of yttrium (Y) to Al-based MGs to enhance the glass-forming ability of this MG, which was then used for dealloying to successfully fabricate the nanoporous structures (see Figure 3i).[106] Inoue et al. explored pseudobinary

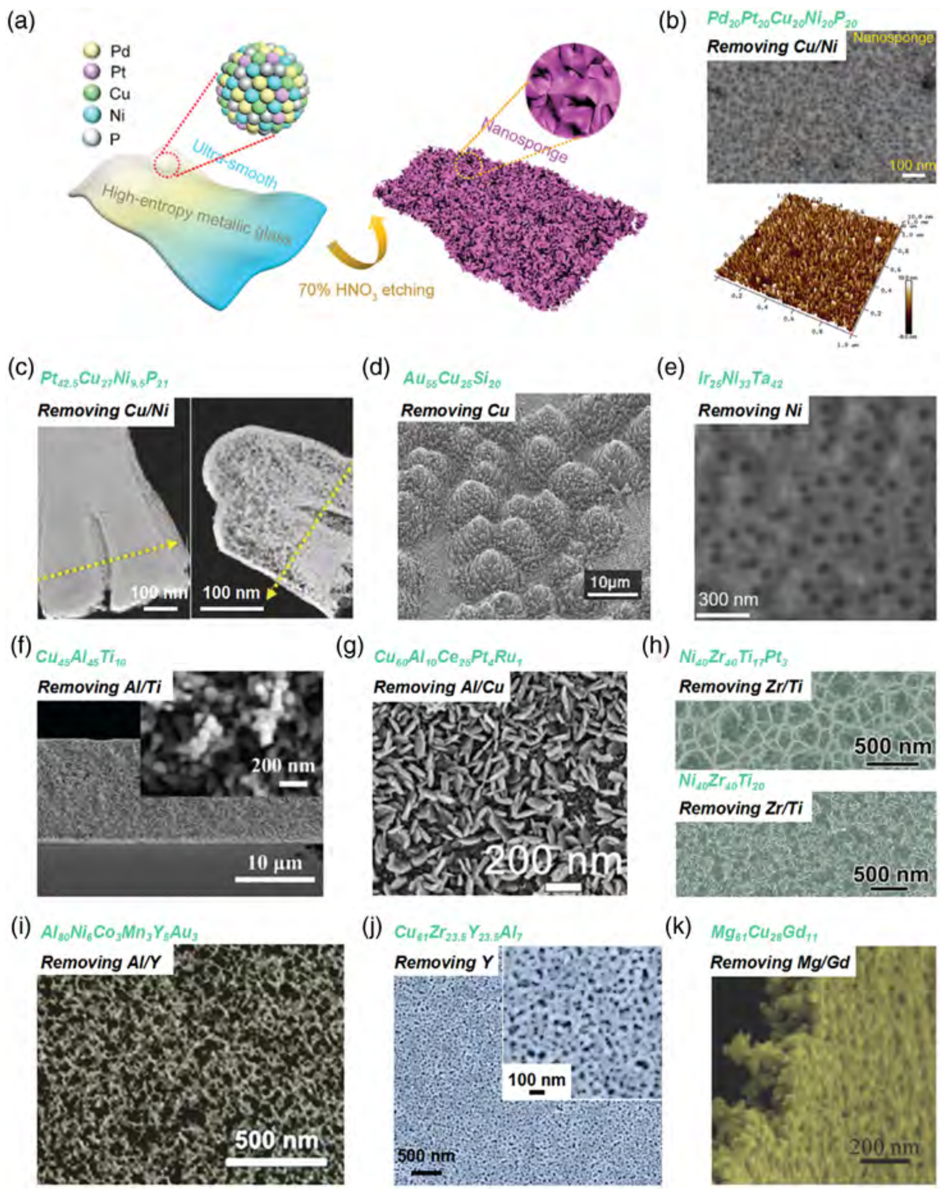

Figure 3. Fabrication of MGs with nanostructures by dealloying process. a) The schematic diagram for fabricating MGs with nanostructures by dealloying. Reproduced with permission.[98] Copyright 2021, Wiley-VCH. b) The porous $Pd_{20}Pt_{20}Cu_{20}Ni_{20}P_{20}$ high-entropy MGs. Reproduced with permission.[98] Copyright 2021, Wiley-VCH. c) The porous $Pt_{42.5}Cu_{27}Ni_{9.5}P_{21}$ MG. Reproduced with permission.[99] Copyright 2016, Wiley-VCH. d) The porous $Au_{55}Cu_{25}Si_{20}$ MG. Reproduced with permission.[100] Copyright 2018, The Royal Society of Chemistry. e) The porous $Ir_{25}Ni_{33}Ta_{42}$ MG. Reproduced with permission.[102] Copyright 2022, Elsevier. f) The porous $Cu_{45}Al_{45}Ti_{10}$ MG. Reproduced with permission.[103] Copyright 2020, Taylor & Francis. g) The nanosheets of $Cu_{60}Al_{10}Ce_{25}Pt_4Ru_1$ MG. Reproduced with permission.[104] Copyright 2022, Elsevier. h) The porous $Ni_{40}Zr_{40}Ti_{17}Pt_3$ and $Ni_{40}Zr_{40}Ti_{20}$ MG. Reproduced with permission.[105] Copyright 2019, Wiley-VCH. i) The porous $Al_{80}Ni_6Co_3Mn_3Y_5Au_3$ MG. Reproduced with permission.[106] Copyright 2020, The Royal Society of Chemistry. j) The porous $Cu_{61}Zr_{23.5}Y_{23.5}Al_7$ MG. Reproduced with permission.[107] Copyright 2021, Springer. k) The porous $Mg_{61}Cu_{28}Gd_{11}$ MG. Reproduced with permission.[108] Copyright 2021, Elsevier.

$Cu_{46}Zr_{23.5}Y_{23.5}Al_7$ MG and then removed the rare-earth elements inside the MG to also form nanopores (see Figure 3j).[107] Zhang et al. synthetized Cu nanoporous films with a thickness of ≈200 nm by dealloying magnesium (Mg) and gadolinium (Gd) on the outer surface of thick $Mg_{61}Cu_{28}Gd_{11}$ MGs (see Figure 3k). They found that local reaction latent heat-induced glass transition played a key role in the formation of MGs with nanostructures.[108] In summary, although the dealloying process fills a gap in porous nanostructures on MGs, safety concerns in the fabrication process and how the chemical solution is handled still need to be considered.

2.3. Other Nanoengineering Techniques

With the exception of TPF and dealloying, both widely used nanoengineering for fabricating the MGs with nanostructures. A number of methods inspired by traditional nanomaterials have also been developed to the MGs with nanostructures. We focus on these novel nanoengineering and the advantages of their corresponding MGs with nanostructures in this section.

Electrospinning as an advanced processing technique that first appeared in 1914.[109] After a comprehensive assessment of the complexity and economy of the process to form nanostructures, Jung et al. applied this method for MGs to fabricate nanofibers with the diameter of $\approx$200 nm (see **Figure 4**a).[110] These nanofibers have an interlocking arrangement, which contributes to the numerous pore channels and the large specific surface area of the MGs with nanostructures. Gas atomization is also a novel technique for forming fine fibers of MGs with nanostructures. Inoue et al. formed MG nanowires with different components using gas atomization after fluid dynamics calculations, while they also predicted the aspect ratio of nanowires that could be formed by some noble metal-based MGs in that way (see Figure 4b).[111] The combination of selective corrosion and passivation is a new idea for fabricating porous MGs provided by Cheng et al (see Figure 4c).[112] The ingenious feature of this method is that the formation of a passivated layer on a particular MG prevents further corrosion, thus preserving the original disordered atomic structure of MGs, which is not available with dealloying process. Liu et al. explored MGs with nanostructures with tunable composition and shape, using a combination of turntable oblique angle deposition and magnetron sputtering. The variation of the target material in the magnetron sputtering system and the change of the tilt angle during the formation of this approach is key to achieving multicomponent and complex shaped structures for MGs with nanostructures (see Figure 4d).[113] Besides magnetron sputtering, a physical vapor deposition (PVD) method, chemical vapor deposition (CVD) has also been utilized in the fabrication of MGs with nanostructures by Doubek et al (see Figure 4e).[99] They initially used the TPF process to fabricate large-area nanowires on Pt-based MGs, on the basis of which they then electrodeposited a $\approx$20 nm layer of MnO_x to coat nanowires, and the MGs with nanostructures achieved by this CVD process have also been proven to have good charge storage capacity. Forming MGs with nanostructures in ultrashort times has long been the pursuit of researchers. Ma et al. recently discovered the novel ultrasonic plasticity of MGs under high-frequency ultrasonic vibrations and used the ultrasonic plasticity to fabricate nanowires on the MG surface in a very short time ($<$1 s) (see Figure 4f).[59] This technique improves the current dilemma of the time required to form MGs with nanostructures and opens up the possibility for the commoditization of MGs with nanostructures. Some unique nanoengineering techniques have been used to synthesize the nanoparticles of MGs, including solvothermal synthesis (see Figure 4g),[114] pulsed laser ablation,[115] etc. It is worth noting that Liang et al. successfully fabricated MG nanoparticles using $Fe_{78}Si_9B_{13}$ MGs by picosecond laser ablation in several organic solvents. The chemical state and morphology of the nanoparticles were observed to reveal the corresponding formation mechanism. This provides a new way to synthesize functional MG nanoparticles (see Figure 4h).[116] Moreover, Yan et al. used thermoplastic polymers to coat MGs and fabricate nanoribbons with thicknesses close to 40 nm on a large scale by thermal drawing and demonstrated the many applications of this nanoribbon, which will be described in detail in subsequent sections (see Figure 4i).[117]

A review of the above literature shows that, after many years of research, a number of well-established or novel nanoengineering methods have been used to fabricate MGs with nanostructures. These methods have some unique features in the formation of MGs with nanostructures. **Table 1** compares the pros and cons of different nanoengineering methods for fabricating MGs with nanostructures from the aspects of material sustainability, processing speed, cost, and the controllability of the resulting structure. However, more nanoengineering techniques available for the formation of MGs with nanostructures also need to be explored, and some structural developments at the atomic level are also worth investigating.

3. Functional Applications

3.1. Wettability

The fundamental purpose of MGs with nanostructures is to tackle challenges within certain functional applications or to deliver specific properties in some fields. Many attempts have been made in this regard using carefully designed MGs with nanostructures.

Wettability plays an important role in many fields such as bionics,[118] environment,[119] and energy.[120] It is now generally accepted that the complex and specific surface structure is one of the key factors influencing the wettability, which makes many MGs with nanostructures available for wettability research. Along with a review of some methods in which MGs with nanostructures can be fabricated, we also summarized some applications for MGs with nanostructures in terms of their wettability. A micro-/nanostructure on Pd-based MGs with superior mechanical stability and corrosion resistance has been designed by Ma et al. The surface has an increased CA of nearly 100° compared with the original polished surface, demonstrating superhydrophobic properties, and also exhibits excellent water droplet adhesion properties at 90° and 180° inclinations (see **Figure 5**a).[90] In another work by Ma et al., they also investigated how the wettability changed after the formation of nanowires on this MG surface. Unlike the wettability of the micro-/nanostructures described above, when the nanowires were fabricated in the MG surface, the otherwise hydrophilic surface also became more hydrophilic; they suggest that the presence of the nanowires provided more space for water to penetrate, which was a key mechanism for the change in wettability. In addition, the bubble release performance of the surfaces with nanowires underwater is also investigated in this previous work and they observed that the presence of nanowires enhanced bubble release (see Figure 5b).[78] Sun et al. formed hierarchical structures by vapor deposition of MGs into the butterfly wing surface. This hierarchical structure perfectly replicated the skeleton of the butterfly wing surface with a hydrophobic CA close to 140° (see Figure 5c).[121] Some investigations have also been carried out on this application by Hasan et al. They formed some hierarchical structure on the MG surface by the TPF process and systematically observed their wettability (see Figure 5d).[89] Besides

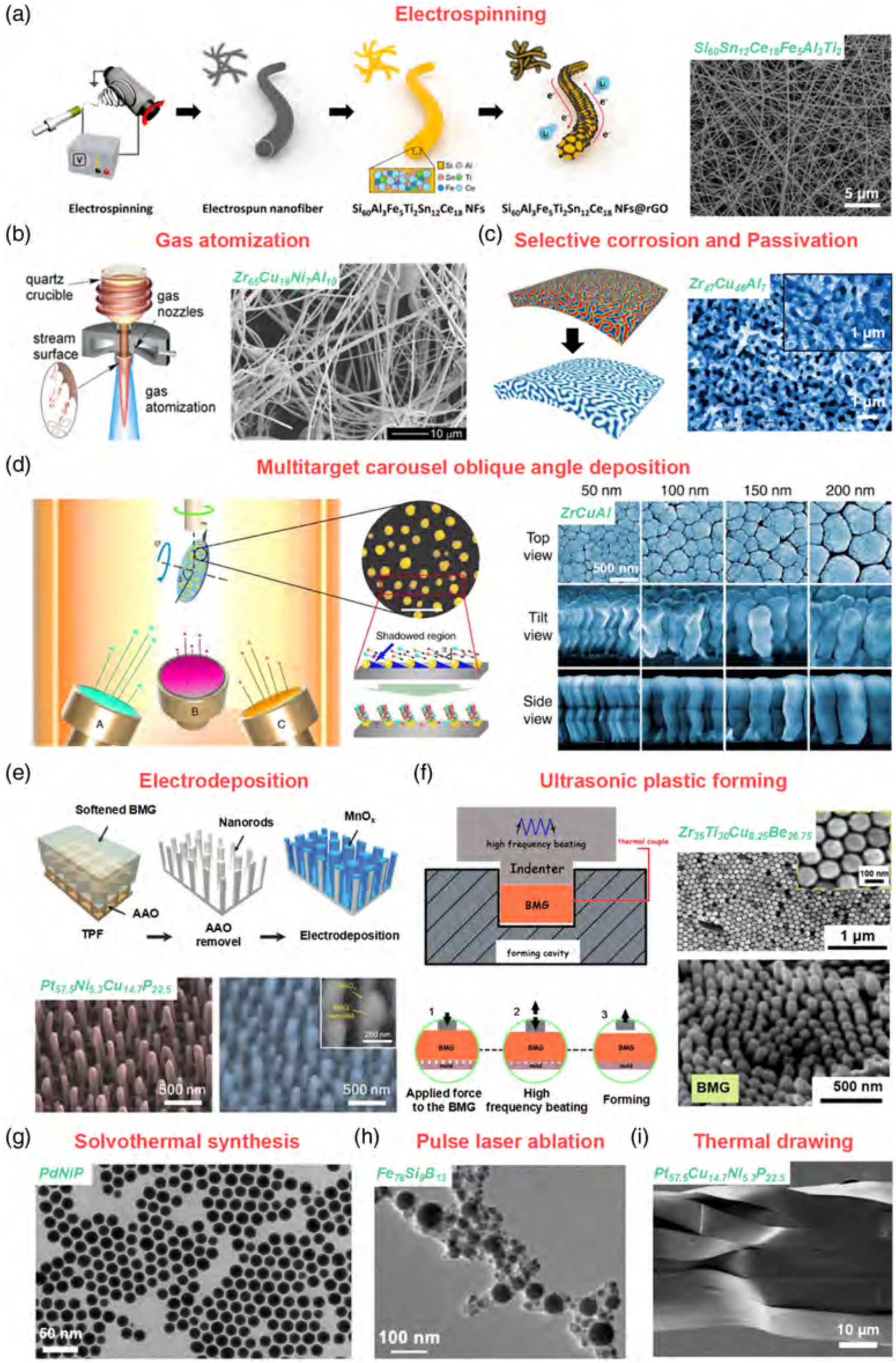

Figure 4. The other ways to fabricate the MGs with nanostructures. a) Electrospinning. Reproduced with permission.[110] Copyright 2015, American Chemical Society. b) Gas atomization. Reproduced with permission.[111] Copyright 2012, American Chemical Society. c) Selective corrosion and passivation. Reproduced with permission.[112] Copyright 2017, American Chemical Society. d) Multitarget carousel oblique angle deposition. Reproduced with permission.[113] Copyright 2015, Nature Publishing Group. e) Electrodeposition. Reproduced with permission.[99] Copyright 2016, Wiley-VCH. f) Ultrasonic plastic forming. Reproduced with permission.[59] Copyright 2015, Nature Publishing Group. g) Solvothermal synthesis. Reproduced with permission.[114] Copyright 2014, American Chemical Society. h) Pulse laser ablation. Reproduced with permission.[116] Copyright 2021, Elsevier. i) Thermal drawing. Reproduced with permission.[117] Copyright 2020, Nature Publishing Group.

Table 1. A summary about the pros and cons of different nanoengineering for forming the MGs with nanostructures.

Methods	Suitability	Processing speed	Cost	Controllability	Ref.
TPF	MGs with excellent TPF ability	Fast	Low	High	[47,78,81]
Dealloying	MGs with dissolved elements	Slow	Low	Low	[98,99]
Magnetron sputtering	Most MGs	Slow	Middle	High	[113,121]
UPF	Most MGs	Fast	Low	High	[59]
Gas atomization	Most MGs	Middle	Middle	Low	[111]
Pulse laser ablation	Most MGs	Fast	Middle	Low	[116,155]
Thermoplastic drawing	MGs with excellent TPF ability	Fast	Low	Middle	[117,156]
Electrospinning	Most MGs	Middle	Middle	Low	[110]
Solvothermal synthesis	Most MGs	Slow	High	High	[114]
Electrodeposition	Most MGs	Middle	Low	High	[157]

studies on designing micro-/nanostructures on MGs to change their surface wettability, some recent studies on using external factors to regulate the wettability of MGs with nanostructures are also worthy to be summarized. Liu et al. proposed a way to form periodic and crumpled MGs with nanostructures by stretching MGs films, and the wettability of the surface and the size of the characteristic nanostructures can be regulated by prestrains (see Figure 5e).[122] In another study, Chen et al. used a combination of photoresist hole arrays and sputter deposition technique to fabricate large-area and tunable diameter MGs nanotubes. When voltage was applied to the sides of the surface with nanotubes, the wettability was regulated according to the voltage exchange, and they also examined the adhesion of the nanotubes (see Figure 5f).[123] These studies about wettability open up new routes for the application of MGs with nanostructures and also provide a practical reference for further research on MGs with nanostructures in other areas.

3.2. Catalysis

Nanowires,[124] nanoparticles,[115] nanopores,[125] and other nanostructures formed by the aforementioned nanoengineering techniques show a strong specific surface area and a large number of active sites, which make MGs with nanostructures relevant for some catalytic reactions (see **Figure 6**a). MGs with nanostructures as a catalyst for the most common hydrogen evolution reaction (HER) and oxygen evolution reaction (OER) were validated in previous work. For example, Johny et al. performed high-entropy MGs nanoparticles containing different amounts of molybdenum (Mo) for OER and found that these high-entropy MG nanoparticles have excellent OER catalytic properties. They also pointed out that a small amount of Mo enhanced their catalytic efficiency of OER under the same conditions, which was attributed to the addition of Mo increasing the crystalline spacing between the amorphous phases (see Figure 6b).[115] The process used to produce hydrogen following the deposition of nanoparticles on MG nanowires can be clearly seen in Figure 6c, and the synthesis of this catalyst was done by Ma et al. They found that this catalyst had catalytic properties in 0.5 M H_2SO_4 solution comparable with that of commercial 10% Pt/C catalysts and could achieve sustained operation for up to 500 h.[78] Besides MGs with nano-structures for HER in acidic solutions, Jia et al. also achieved hydrogen evolution efficiencies similar to those of commercial 20% Pt/C using porous high-entropy MGs in alkaline solutions (see Figure 6d).[98] They have also explored non-noble metal-based MGs that can be used in alkaline environments for water oxidation reactions. After a simple hydroxylation process, they achieved nanoscale heterogeneities on the $Fe_{50}Ni_{30}P_{13}C_7$ MG surface; this catalyst showed excellent industrial-level water oxidation performance.[126] Carmo et al. explored MGs with nanostructures as catalysts for novel catalytic reactions. They found that Pt-based MG nanowires without any treatment could oxidize carbon monoxide, methanol, and ethanol and that the oxidation efficiency was dependent on the diameter of the nanowires, with the highest oxidation efficiency achieved when the diameter of the nanowires was reduced by 13 nm (see Figure 6e).[127] In addition, MGs with nanostructures can be employed in the electrodes of some fuel cells or lithium-ion batteries. Taylor et al. showed the application of hierarchical MGs from nanostructures to fuel cells. They used MGs with nanostructures as the most critical catalytic electrode plate in the cell and then prepared a miniature fuel cell through a series of assemblies (see Figure 6f), which were tested to demonstrate the feasibility of MGs with nanostructures for fuel cells.[88] Kim et al. fabricated a nanostructure with high electron transport capacity by coating amorphous nanofibers with graphene, which exhibited excellent charge/discharge cycling properties when used as the anode of a lithium-ion battery (see Figure 6g).[110] MGs recently made a significant impression in the environmental field as a new type of catalyst.[128–132] For example, some reports demonstrate that single-$Co_{78}Si_8B_{14}$ MG can be used for direct wastewater degradation,[133] regulating the elemental boron (B) content of iron (Fe)-based MGs that can enhance electron delocalization to improve degradation performance for multiple organic pollutants,[134] the MG 3D structures forming by 3D printing technology that can improve reusability in wastewater treatment,[135] and elevating the annealing temperature of MGs that can restore its catalytic performance for dye degradation,[129] etc. Some MGs with nanostructures have also exhibited robust advantages in this functional applications. Jia et al. demonstrated an efficient and reusable MG catalyst for the degradation of organic pollutants and found that

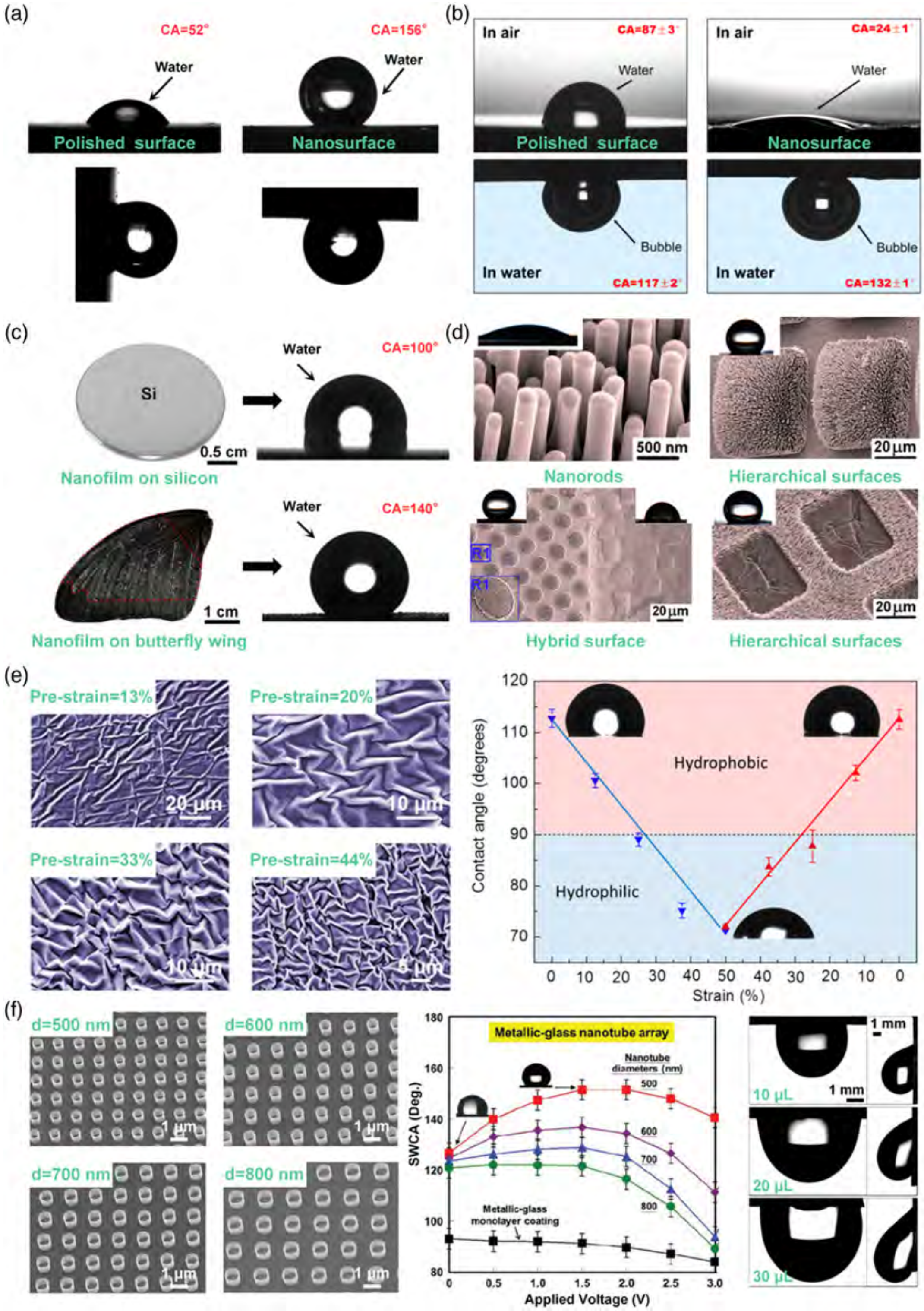

Figure 5. The application of MGs with nanostructures in wettability. a) The hierarchical surface. Reproduced with permission.[90] Copyright 2014, AIP. b) Nanowires. Reproduced with permission.[78] Copyright 2021, The Royal Society of Chemistry. c) The hierarchical surface. Reproduced with permission.[121] Copyright 2019, Springer. d) The hierarchical surface. Reproduced with permission.[89] Copyright 2015, American Chemical Society. e) Crumpled nanostructure. Reproduced with permission.[122] Copyright 2018, IOP Publishing. f) Nanotubes. Reproduced with permission.[123] Copyright 2018, The Royal Society of Chemistry.

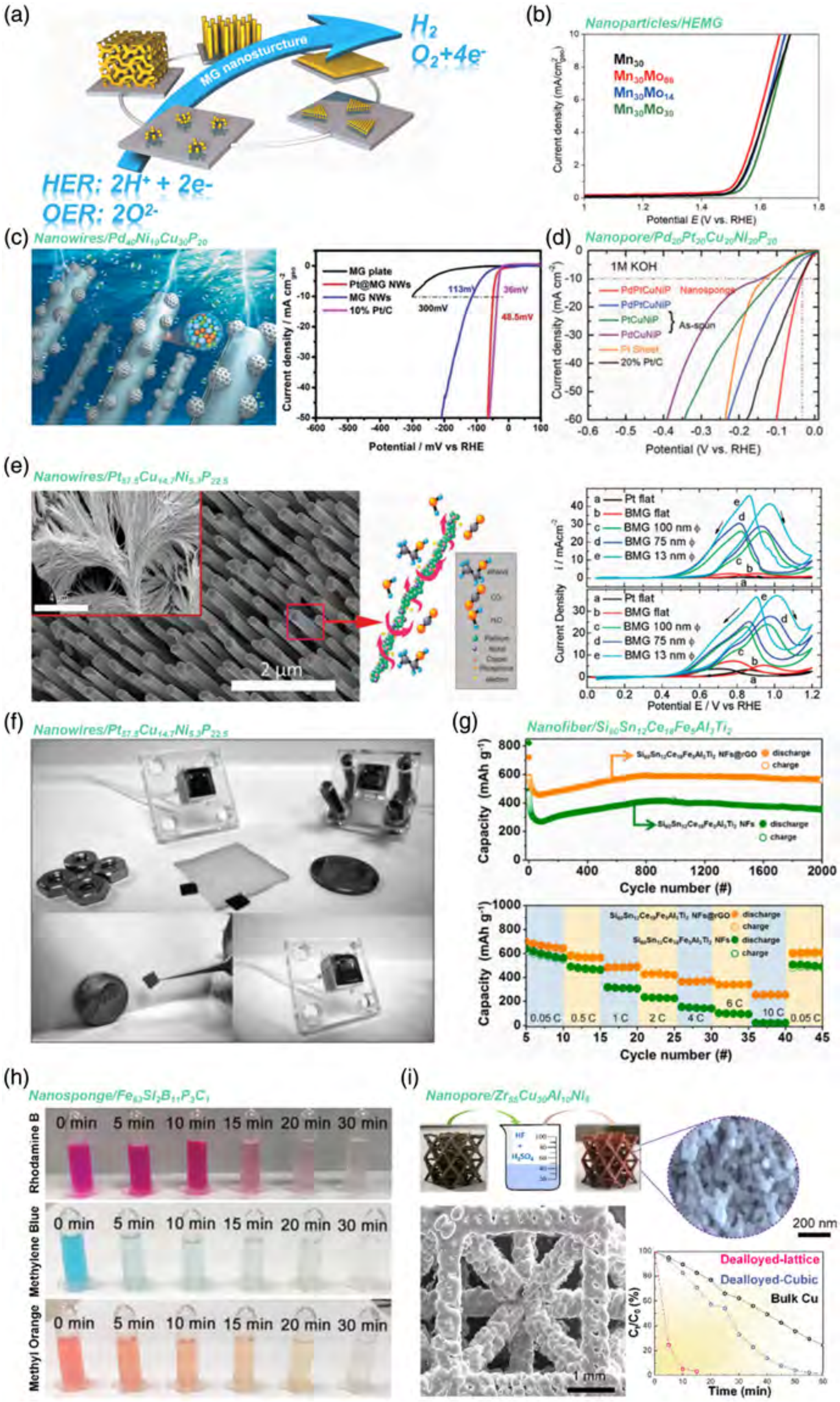

Figure 6. The electrochemical application of MGs with nanostructures. a) The schematic diagram of MGs with nanostructures for electrochemical applications. Reproduced with permission.[154] Copyright 2014, American Chemical Society. b) Nanoparticles for OER. Reproduced with permission.[115] Copyright 2022, Springer. c) Nanowires for HER. Reproduced with permission.[78] Copyright 2021, The Royal Society of Chemistry. d) Nanopores for HER. Reproduced with permission.[98] Copyright 2021, Wiley-VCH. e) Nanowires for methanol and ethanol oxidation. Reproduced with permission.[127] Copyright 2011, American Chemical Society. f) Nanowires for fuel cell. Reproduced with permission.[88] Copyright 2013, Wiley-VCH. g) Nanofibers for lithium-ion battery. Reproduced with permission.[110] Copyright 2015, American Chemical Society. h) Porous sponge for wastewater remediation. Reproduced with permission.[136] Copyright 2019, Wiley-VCH. i) 3D printing structures with nanopores for degradation. Reproduced with permission.[137] Copyright 2018, Elsevier.

self-reconstructed nanoporous layers and amorphous oxide interlayers on the MG surface were key to the efficiency and stability of the catalyst (see Figure 6h).[136] Liu et al. also made pioneering attempts in this application. They created 3D components with lattice structures using the Zr-based MG by 3D printing and then dealloyed it to form a nanoporous structure on their surface. This lattice with nanoporous structures has a more efficient degradation of methyl orange than the dealloyed cubes and bulk Cu (see Figure 6i).[137] Not all MGs with nanostructures can be utilized for some common catalytic reactions. Specific catalytic reactions can be selected with the consideration of the main elements contained in the MGs with nanostructures itself, and in general, MGs with nanostructures can be used as containers for storing nanoparticles or atoms to achieve efficient catalytic performance synergizing with nanostructures.

3.3. Other Applications

MGs with nanostructures can also be developed for a number of other functional applications. Kumar formed nanowires into BMGs by the TPF process, and then the BMGs with nanowires were crystallized at a temperature above the T_x, thus preparing a nanomold that can serve at a wide range of temperatures. **Figure 7**a depicts a process and confirms the practicality of the nanomold on PMMA and the same BMG to form nanoholes.[47] In optics, there has been some previous work that has found that the presence of nano- or microstructures will alter the movement of light, which directly affects the optical properties of its surface.[69,85,138,139] Inspired by this, Yao et al. successfully fabricated numerous photonic crystals on a large-area MG surface. Compared with the structural color of the Si template and the formed MG surface at different angles, they found that both exhibited the same color (Figure 7b).[86] Schroers et al. conducted a great deal of research in biomedicine involving the MGs with nanostructures, including cellular response,[140,141] cell fusion,[142] cell polarisation,[143] and more.[144] Here we have listed one of their major works in biomedicine, where they found that different diameters of Pt-based MG nanowires can trigger different types of cellular responses, for example, fibroblasts can detect the presence of 55 nm-diameter Pt-based MG nanowires, while macrophages respond to 200 nm-diameter Pt-based MG nanowires. The significance of this work is that it provides guidance for the application of MGs with nanostructures in the biological field (see Figure 7c).[140] The applications of MGs with nanostructures for neuroscience have also been recently demonstrated by Yan et al. As mentioned earlier, they used thermal drawing to process MGs that can be fabricated into micro or nanofibres, which were then implanted into the brains of rats for long-term recording and neural stimulation, and the longevity of the nanofibres in the rat was evaluated (see Figure 7d). Notably, they also showed the application of these nanofibres to optoelectronics.[117]

4. Conclusion and Future Perspectives

In recent years, MGs with nanostructures have gained momentum and are becoming an important research area in the field of MGs. Unique structures such as nanowires, nanopores, and nanoparticles have been fabricated by nanoengineering, and each of these nanostructures also exhibits different properties to suit functional applications within the fields of wettability, bioscience and catalysis, etc. The dimensionality and the corresponding functional applications for the individual MGs with nanostructures fabricated by nanoengineering have been summarized in **Table 2**. However, after reviewing these nanoengineering approaches and the applications for MGs with nanostructures, we have noted some challenges for MGs with nanostructures that still need to be tackled. These include the optimization of nanoengineering and the exploration of potential functional applications involving MGs with nanostructures. To tackle these challenges, we propose a few instructive insights.

4.1. The Development of MG Composition

The table shows that the majority of MGs used for TPF process are noble metal based MGs. The main reason is that noble metal-based MGs have excellent resistance to oxidation at high temperatures and are less likely to form oxide layers on the MG surface to prevent the forming of MGs with nanostructures. However, these compositions of MGs are not conducive to the development of various MGs with nanostructures for commercial applications. On this basis, high-throughput development of non-noble metal-based MGs that resist oxidation at high temperatures or the manufacture of ultrahigh-vacuum TPF equipment would greatly improve this situation.

4.2. The Exploration of Facile, Economical, and Environmentally Friendly Templates

AAO and Si templates are common nanoforming templates for the TPF process, and the removal is often achieved by chemical corrosion. However, chemical solutions with different solubility and corrosion times will affect the extent to which the surface templates can be removed, and this process involving corrosive solutions can be dangerous. In addition, these templates only can be used to form single nanoarrays due to processing limitations. In this context, the new templates that are soluble, environmentally friendly, and that can form irregular 3D structures such as hierachical pores and arrays is also worth investigating. Developing templates for forming atomic structures of MGs is also promising.

4.3. Potential Functional Applications for MGs with Nanostructures

Some potential application possibilities for MGs with nanostructures can be predicted from the morphological characteristics of the nanostructures and the composition of the MGs with nanostructures. Manufacturing MG with nanostructures for potential applications such as radiation cooling, light absorbers, seawater desalination, and drug injection is highly desired. Moreover, various applications can be developed based on specific MG compositions, for example, rare earth-based MGs with nanostructures for tail gas treatment, MGs with nanostructures containing the elements antimony (Sb) and tin (Sn) for sodium

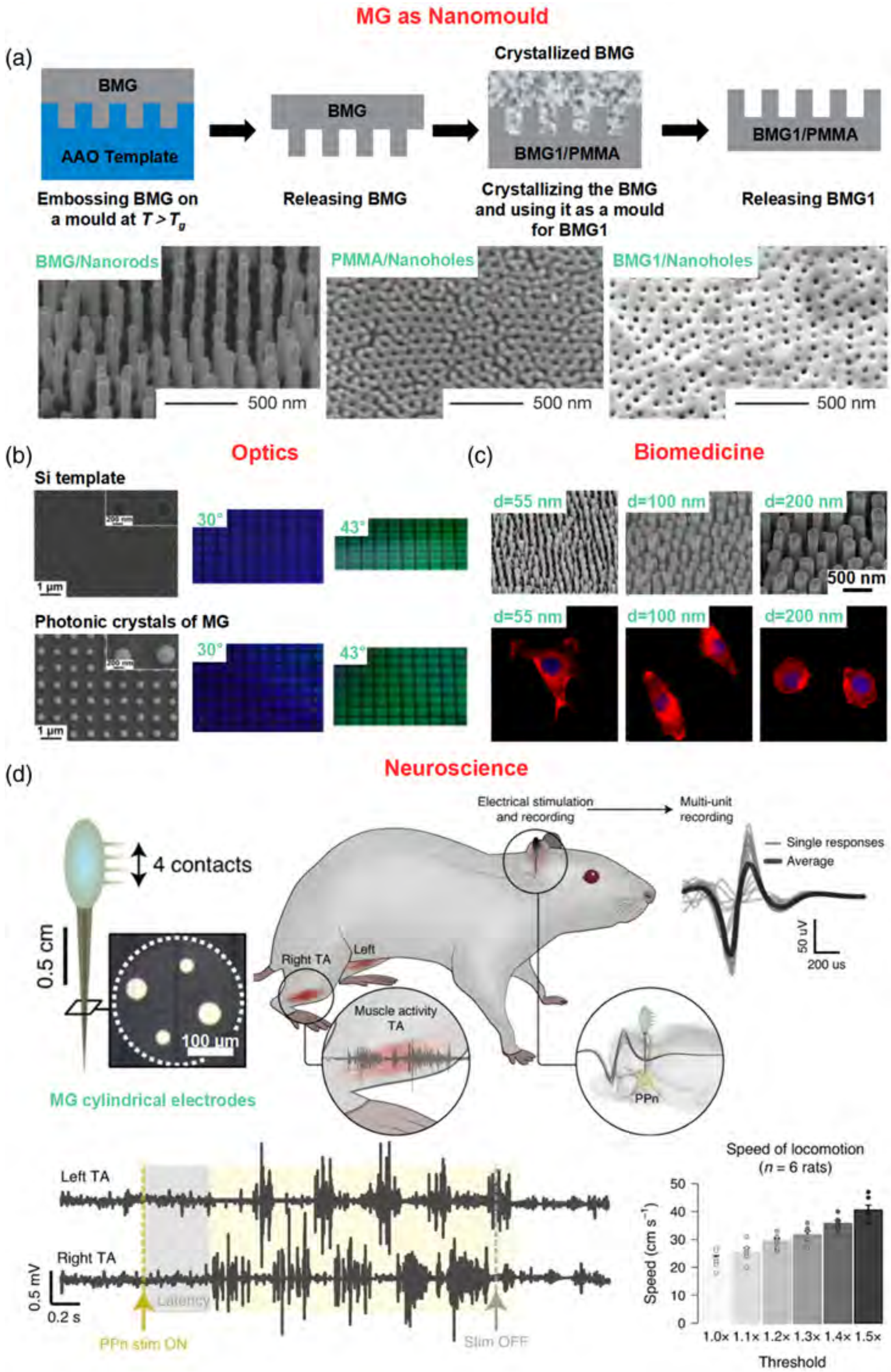

Figure 7. The other applications of MGs with nanostructures. a) MG with nanostructure as a nanomold. Reproduced with permission.[47] Copyright 2009, Nature Publishing Group. b) Optics. Reproduced with permission.[86] Copyright 2015, Elsevier. c) Biomedicine. Reproduced with permission.[140] Copyright 2014, American Chemical Society. d) Neuroscience. Reproduced with permission.[117] Copyright 2020, Nature Publishing Group.

(Na) storage, Mg-based MGs with nanostructures for drug delivery in living organisms, etc.

We believe that our review will provide some insight into those who are working on MGs with nanostructures and to some interdisciplinary researchers. Finally, we are grateful to the research communities that have made outstanding contributions to the field of MGs with nanostructures.

Table 2. The summary of the nanoengineering for forming MGs with nanostructures, the formed sizes, and the functional applications for these MGs with nano-structures.

Composition	Fabrication method	Formed structures	Forming size	Functional applications	Ref.
$Pd_{40}Ni_{10}Cu_{30}P_{20}$	TPF	Nanowires	≈300 nm	Electrochemical applications	[78]
$Pt_{57.5}Cu_{14.7}Ni_{5.3}P_{22.5}$	TPF	Nanowires, Nano-holes	13, 35, 55 nm	MG mold	[47]
$Pt_{57.5}Cu_{14.7}Ni_{5.3}P_{22.5}$	TPF	Nanowires	≈250 nm	Fuel cell	[88]
$Pt_{57.5}Cu_{14.7}Ni_{5.3}P_{22.5}$	TPF	Nanowires	≈100 nm	Electrochemical applications	[127]
$La_{55}Al_{25}Ni_{15}Cu_{10}Co_5$, $Pt_{57.5}Cu_{14.7}Ni_{5.3}P_{22.5}$	TPF	Nanowires	≈200 , ≈300 nm	–	[158]
$La_{55}Al_{25}Ni_{15}Cu_{10}Co_5$	TPF	Nanowires	≈330, ≈290, ≈170 nm	Wettability	[83]
$Ni_{60}Pd_{20}P_{17}B_3$	Cyclic voltammetry	Dendritic nanostructure	–	Electrochemical applications	[159]
$Ni_{60}Pd_{20}P_{17}B_3$	TPF	Nanowires	≈200 nm	–	[159]
$Pd_{43}Ni_{10}Cu_{27}P_{20}$	TPF	Nanowires	≈20 nm	Electrochemical applications	[124]
$Au_{49}Ag_{5.5}Pd_{2.3}Cu_{26.9}Si_{16.3}$	TPF	Nano-stripes	≈453 nm	–	[160]
$Pd_{40.5}Ni_{40.5}P_{19}$	TPF	Nanowires	≈55 nm	–	[81]
$Pd_{40.5}Ni_{40.5}P_{19}$	TPF	Nanowires	≈55 nm	Enhanced Raman scattering	[161]
$Zr_{35}Ti_{30}Be_{26.75}Cu_{8.25}$	TPF/ecthing	Nano protrusion	≈10–30 nm	Wettability	[162]
$Pd_{40}Ni_{10}Cu_{30}P_{20}$	TPF	Nano protrusion	≈80–100 nm	Wettability	[90]
$Pt_{57.5}Cu_{14.7}Ni_{5.3}P_{22.5}$	TPF	Nanowires	100, 150, 200 nm	Wettability	[89]
$Pt_{57.5}Cu_{14.7}Ni_{5.3}P_{22.5}$	TPF	Nanowires	55, 100, 150, 200 nm	Biomedical applications	[140]
$Pt_{57.5}Cu_{14.7}Ni_{5.3}P_{22.5}$	TPF	Nanowires	55 nm	Biomedical applications	[143]
$Pt_{57.5}Cu_{14.7}Ni_{5.3}P_{22.5}$	TPF	Nanowires	55, 100, 150, 200 nm	Biomedical applications	[142]
$Pt_{57.5}Cu_{14.7}Ni_{5.3}P_{22.5}$	TPF	Nanowires	200 nm	Biomedical applications	[144]
$Pt_{57.5}Cu_{14.7}Ni_{5.3}P_{22.5}$	TPF	Nanowires	200 nm	Biosensors	[163]
$Fe_{40}Co_{20}Ni_{15}P_{10}C_{10}B_5$	TPF	Nano-pattern	300 nm	–	[164]
$Pd_{40.5}Ni_{40.5}Si_{4.5}P_{14.5}$	TPF	Photonic crystals	350 nm	Optical and mold applications	[86]
$Pt_{57.5}Cu_{14.7}Ni_{5.3}P_{22.5}$	TPF	Nanowires	40 nm	Biomedical applications and Wettability	[141]
$Pd_{42.5}Cu_{30}Ni_{7.5}P_{20}$	TPF	Nano-holes	30 nm	–	[87]
$Ti_{41.5}Cu_{42.5}Zr_{2.5}Ni_{7.5}Hf_5Si_1$	TPF	Nano-holes Nano-pattern	110, 500 nm	–	[165]
$Pd_{40}Ni_{40}P_{20}$	TPF	Nano-gratings	150, 655 nm	Optical applications	[85]
$Ti_{45}Zr_{20}Be_{30}Fe_5$	TPF	Nanorods	400 nm	–	[166]
$Ti_{41}Zr_{25}Be_{28}Fe_6$	TPF	Nanorods	400 nm	–	[84]
$Zr_{35}Ti_{30}Cu_{8.25}Be_{26.75}$ $Zr_{44}Ti_{11}Cu_{10}Ni_{10}Be_{25}$ $Mg_{65}Cu_{25}Y_{10}$	TPF	Nanowires	200 nm	–	[82]
$Pt_{57.5}Cu_{14.7}Ni_{5.3}P_{22.5}$ $Pd_{43}Ni_{10}Cu_{27}P_{20}$	TPF	Nanowires	40-200 nm	–	[77]
$Pt_{57.5}Cu_{14.7}Ni_{5.3}P_{22.5}$	TPF	Nanowires	100 ± 20 nm	–	[167]
$(Zr_{50.7}Cu_{28}Ni_9Al_{12.3})_{98.5}Y_{1.5}$	TPF	Nanowires	300, 390 nm	Wettability	[168]
$Pt_{57.5}Cu_{14.7}Ni_{5.3}P_{22.5}$ $Au_{49}Ag_{5.5}Pd_{2.3}Cu_{26.9}Si_{16.3}$	Thermal drawing	Nano-ribbons	40 nm	Optoelectronic and neuroscience	[117]
$Pt_{57.5}Cu_{14.7}Ni_{5.3}P_{22.5}$ $Pd_{43}Cu_{27}Ni_{10}P_{20}$ $Ni_{60}Pd_{20}P_{17}B_3$ $Zr_{35}Ti_{30}Cu_{8.25}Be_{26.75}$	Thermoplastic drawing	Nano-tips, Nanowires, Nano-tubes	≈500 nm	Mechanical applications	[156]
$Ni_{40}Zr_{40}Ti_{17}Pt_3$ $Ni_{40}Zr_{40}Ti_{20}$	Dealloying	Nano-pore	–	Electrochemical applications	[105]
$Fe_{29}Co_{27}Ni_{23}Si_9B_{12}$	Etching	Nano-pits	–	Electrochemical applications	[169]
PdNiP	Solvothermal synthesis	Nano-particles	6–17 nm	Electrochemical applications	[114]

Table 2. Continued.

Composition	Fabrication method	Formed structures	Forming size	Functional applications	Ref.
$Pd_{20}Pt_{20}Cu_{20}Ni_{20}P_{20}$	Dealloying	Nano-pore	≈10 nm	Electrochemical applications	[98]
$Mg_{61}Cu_{28}Gd_{11}$ $Mg_{61}Cu_{21}Ag_{7}Gd_{11}$ $Mg_{61}Cu_{14}Ag_{14}Gd_{11}$	Dealloying	Nanoporous films	≈25 nm, ≈30, ≈35 nm	–	[108]
$Fe_{35}Ni_{35}Co_{8}Al_{2}P_{20}$	Dealloying	Nano-pore	10–200 nm	Electrochemical applications	[170]
$Cu_{45}Al_{45}Ti_{10}$	Dealloying	Nano-pore	39–79 nm	Degradation applications	[103]
$Al_{82}Ni_{6}Co_{3}Mn_{3}Y_{3}Au_{3}$	Dealloying	Nano-pore	<100 nm	Electrochemical applications	[125]
$Ni_{25}Y_{60}Al_{15}$	Dealloying	Nanopore	5–20 nm	Electrochemical applications	[171]
$Cu_{60}Al_{10}Ce_{25}Pt_{4}Ru_{1}$	Dealloying	Nanosheets	60 × 120 nm–150 × 270 nm	Electrochemical applications	[104]
$Ir_{25}Ni_{33}Ta_{42}$	Dealloying	Nano-pore	20–40 nm	Electrochemical applications	[102]
$Pt_{42.5}Cu_{27}Ni_{9.5}P_{21}$	Dealloying	Nano-arrays with mesopore	–	Electrochemical applications	[99]
$Al_{80}Ni_{6}Co_{3}Mn_{3}Y_{5}Au_{3}$	Dealloying	Nano-pore	10 nm	Electrochemical applications	[106]
$Au_{55}Cu_{25}Si_{20}$	Dealloying	Nano-pore	5–10 nm	Electrochemical applications	[100]
$Zr_{55}Cu_{30}Al_{10}Ni_{5}$	Dealloying	Nanoporous structure	60 nm	Degradation applications	[137]
$Fe_{40}Ni_{20}Co_{20}P_{15}C_{5}$	Dealloying	Nanoporous structure	–	Electrochemical applications	[172]
$Cu_{61}Zr_{23.5}Y_{23.5}Al_{7}$	Dealloying	Nanoporous structure	10–30 nm	Flexible electronics	[107]
NiP	deposition	Nanoporous structure	≈100	Electrochemical applications	[173]
$Fe_{54}Ni_{25}Co_{5}Nb_{6}B_{9}Cu_{1}$ $Fe_{54}Ni_{20}Co_{10}Nb_{6}B_{9}Cu_{1}$ $Fe_{54}Ni_{15}Co_{15}Nb_{6}B_{9}Cu_{1}$	Selective dissolution	Nano-pore	100–300 nm	Electrochemical applications	[174]
$Zr_{47}Cu_{46}Al_{7}$	Selective corrosion and Passivation	Nano-pore	≈25 nm	Hydrogen uptake	[112]
$Zr_{35}Ti_{30}Cu_{8.25}Be_{26.75}$	UPF	Nanowires	80–100 nm	–	[59]
ZrCuAl	Carousel oblique angle deposition	Nano architectures	50, 100, 150, 200 nm	–	[113]
$Zr_{65}Cu_{18}Ni_{7}Al_{10}$ $Fe_{76}Si_{9.6}B_{8.4}P_{6}$	Gas atomization	Nanowires	50–2000 nm	–	[111]
$Cr_{17.5}Co_{17.5}Fe_{17.5}Ni_{17.5}Mn_{30}Cr_{16}Co_{16}$ $Fe_{16}Ni_{16}Mn_{30}Mo_{6}Cr_{14}Co_{14}Fe_{14}Ni_{14}Mn_{30}$ $Mo_{14}Cr_{10}Co_{10}Fe_{10}Ni_{10}Mn_{30}Mo_{30}$	Pulse laser ablation	Nano-particles	22 ± 9 nm 22 ± 16 nm 15 ± 14 nm 14 ± 6 nm	Electrochemical applications	[115]
$Fe_{78}Si_{9}B_{13}$	Pulsed laser ablation	Nano-particle	10–54 nm	Magnetic applications	[116]
$Ni_{80}P_{20}$, $Ni_{75}Pd_{10}P_{15}$	Electro deposition	Nanowires	120 nm	Electrochemical applications	[157]
NiB	Colloidal synthesis	Nano-particle	74 ± 2 nm	Mechanical applications	[175]
$Zr_{41.2}Ti_{13.8}Cu_{12.5}Ni_{22.5}Be_{10}$	Nanosecond pulse laser ablation	Nanoparticle	30, 100 nm	–	[155]
$(Zr_{46}Cu_{46}Al_{8})_{82}Ag_{18}$	Vapor deposition	Hierarchical nanostructure	250 nm	Enhanced Raman scattering	[121]
$Zr_{55}Cu_{30}Al_{10}Ni_{5}$	Sputter deposition	Nanotubes	500, 600, 700, 800 nm	Artificial nanosucker device Wettability	[123]
$Si_{60}Sn_{12}Ce_{18}Fe_{5}Al_{3}Ti_{2}$	Electrospinning	Nanofibers	100, 200 nm	Electrochemical applications	[110]
$Cu_{50}Zr_{50}$ $Fe_{78}Si_{9}B_{13}$	Deposition	Crumpled nanostructure	<200 nm	Wettability	[122]
$Fe_{83}Si_{2}B_{11}P_{3}C_{1}$	Melt-spinning and Fenton-like reaction	Porous sponge layer and interlayer	≈500, ≈4 nm	Degradation applications	[136]
$Fe_{50}Ni_{30}P_{13}C_{7}$	Hydroxylation process	Plate-like morphology	–	Electrochemical applications	[126]

Acknowledgements

The work was supported by the Key Basic and Applied Research Program of Guangdong Province, China (grant no. 2019B030302010), the NSF of China (grant no. 52122105, 51871157, and 51971150), and the National Key Research and Development Program of China (grant no. 2018YFA0703605). The authors also thank the assistance on microscope observations received from the Electron Microscope Center of the Shenzhen University.

Conflict of Interest

The authors declare no conflict of interest.

Keywords

functional applications, metallic glasses, nanoengineering, nanomaterials

Received: May 5, 2022
Revised: June 27, 2022
Published online:

[1] M. Faraday, *Trans. R. Soc. London* **1857**, 145.
[2] C. Frick, B. Clark, S. Orso, A. Schneider, E. Arzt, *Mater. Sci. Eng., A* **2008**, *489*, 319.
[3] M. Lines, *J. Alloys Compd.* **2008**, *449*, 242.
[4] E. Roduner, *Chem. Soc. Rev.* **2006**, *35*, 583.
[5] L. Zhou, Y. Tan, J. Wang, W. Xu, Y. Yuan, W. Cai, S. Zhu, J. Zhu, *Nat. Photonics* **2016**, *10*, 393.
[6] F. Zhao, X. Zhou, Y. Shi, X. Qian, M. Alexander, X. Zhao, S. Mendez, R. Yang, L. Qu, G. Yu, *Nat. Nanotechnol.* **2018**, *13*, 489.
[7] P. J. Alvarez, C. K. Chan, M. Elimelech, N. J. Halas, D. Villagrán, *Nat. Nanotechnol.* **2018**, *13*, 634.
[8] L. Zhu, M. Gao, C. K. N. Peh, G. W. Ho, *Mater. Horizon* **2018**, *5*, 323.
[9] S. Liu, X. Pan, H. Liu, *Angew. Chem.* **2020**, *132*, 5943.
[10] X. Zhu, W. Feng, J. Chang, Y.-W. Tan, J. Li, M. Chen, Y. Sun, F. Li, *Nat. Commun.* **2016**, *7*, 1.
[11] J. Shao, H. Xie, H. Huang, Z. Li, Z. Sun, Y. Xu, Q. Xiao, X.-F. Yu, Y. Zhao, H. Zhang, *Nat. Commun.* **2016**, *7*, 1.
[12] J. Nam, S. Son, K. S. Park, W. Zou, L. D. Shea, J. J. Moon, *Nat. Rev. Mater.* **2019**, *4*, 398.
[13] X. Zhu, Q. Guo, Y. Sun, S. Chen, J.-Q. Wang, M. Wu, W. Fu, Y. Tang, X. Duan, D. Chen, *Nat. Commun.* **2019**, *10*, 1.
[14] W. Liu, P. Zhai, A. Li, B. Wei, K. Si, Y. Wei, X. Wang, G. Zhu, Q. Chen, X. Gu, *Nat. Commun.* **2022**, *13*, 1.
[15] W. Xu, G. Fan, S. Zhu, Y. Liang, Z. Cui, Z. Li, H. Jiang, S. Wu, F. Cheng, *Adv. Funct. Mater.* **2021**, *31*, 2107333.
[16] H. Xie, X. Xie, G. Hu, Versus. Prabhakaran, S. Saha, L. Gonzalez-Lopez, A. H. Phakatkar, M. Hong, M. Wu, R. Shahbazian-Yassar, *Nat. Energy* **2022**, *7*, 281.
[17] Y. Si, Z. Guo, *Nanoscale* **2015**, *7*, 5922.
[18] Z. Li, J. Ma, *Mater. Today Adv.* **2021**, *12*, 100164.
[19] D. Wang, Q. Sun, M. J. Hokkanen, C. Zhang, F.-Y. Lin, Q. Liu, S.-P. Zhu, T. Zhou, Q. Chang, B. He, *Nature* **2020**, *582*, 55.
[20] L. Feng, S. Li, Y. Li, H. Li, L. Zhang, J. Zhai, Y. Song, B. Liu, L. Jiang, D. Zhu, *Adv. Mater.* **2002**, *14*, 1857.
[21] J. U. Kim, S. Lee, S. J. Kang, T.-i. Kim, *Nanoscale* **2018**, *10*, 21555.
[22] L. Feng, P. Huo, Y. Liang, T. Xu, *Adv. Mater.* **2020**, *32*, 1903787.
[23] J. U. Kim, S. J. Kang, S. Lee, J. Ok, Y. Kim, S. H. Roh, H. Hong, J. K. Kim, H. Chae, S. J. Kwon, *Adv. Funct. Mater.* **2020**, *30*, 2003862.
[24] H. Li, L. Wu, H. Zhang, W. Dai, J. Hao, H. Wu, F. Ren, C. Liu, *ACS Appl. Mater. Interfaces* **2019**, *12*, 4081.
[25] Z. L. Wang, J. Song, *Science* **2006**, *312*, 242.
[26] F.-R. Fan, Z.-Q. Tian, Z. L. Wang, *Nano Energy* **2012**, *1*, 328.
[27] C. Chang, V. H. Tran, J. Wang, Y.-K. Fuh, L. Lin, *Nano Lett.* **2010**, *10*, 726.
[28] S. Fu, W. He, Q. Tang, Z. Wang, W. Liu, Q. Li, C. Shan, L. Long, C. Hu, H. Liu, *Adv. Mater.* **2022**, *34*, 2105882.
[29] M. Jin, Y. Wang, M. Chai, C. Chen, Z. Zhao, T. He, *Adv. Funct. Mater.* **2022**, *32*, 2107499.
[30] D. Zhu, Q.-Y. Zhao, H. Choi, T.-J. Lu, A. E. Dane, D. Englund, K. K. Berggren, *Nat. Nanotechnol.* **2018**, *13*, 596.
[31] W. Li, J. Valentine, *Nano Lett.* **2014**, *14*, 3510.
[32] S. Liu, B. Lu, Q. Zhao, J. Li, T. Gao, Y. Chen, Y. Zhang, Z. Liu, Z. Fan, F. Yang, *Adv. Mater.* **2013**, *25*, 4549.
[33] H. Chhipa, *Environ. Chem. Lett.* **2017**, *15*, 15.
[34] G. Rameshaiah, J. Pallavi, S. Shabnam, *Int. J. Eng. Res. Gen. Sci.* **2015**, *3*, 314.
[35] X. Xin, J. D. Judy, B. B. Sumerlin, Z. He, *Environ. Chem.* **2020**, *17*, 413.
[36] M. Usman, M. Farooq, A. Wakeel, A. Nawaz, S. A. Cheema, H. ur Rehman, I. Ashraf, M. Sanaullah, *Sci. Total Environ.* **2020**, *721*, 137778.
[37] Z. Liu, N. Liu, J. Schroers, *Prog. Mater. Sci.* **2022**, *125*, 100891.
[38] A. Biswas, I. S. Bayer, A. S. Biris, T. Wang, E. Dervishi, F. Faupel, *Adv. Colloid Interface Sci.* **2012**, *170*, 2.
[39] K. Ariga, J. P. Hill, Q. Ji, *PCCP* **2007**, *9*, 2319.
[40] D. Qin, Y. Xia, G. M. Whitesides, *Nat. Protoc.* **2010**, *5*, 491.
[41] S. Zhu, Y. Tang, C. Lin, X. Y. Liu, Y. Lin, *Small Methods* **2021**, *5*, 2001060.
[42] N. Bhattacharjee, C. Parra-Cabrera, Y. T. Kim, A. P. Kuo, A. Folch, *Adv. Mater.* **2018**, *30*, 1800001.
[43] Z. Liu, *Nat. Commun.* **2017**, *8*, 1.
[44] L. Xu, L. Shui, Y. Zhang, Q. Peng, L. Xue, Z. Liu, *Appl. Phys. Express* **2020**, *13*, 036503.
[45] Z. Yan, J. Gao, M. Beresna, J. Zhang, *Adv. Opt. Mater.* **2022**, *10*, 2101676.
[46] Y. Feng, X. Liu, K. Li, F. Gong, J. Shen, Y. Lou, *ACS Appl. Mater. Interfaces* **2021**, *13*, 16968.
[47] G. Kumar, H. X. Tang, J. Schroers, *Nature* **2009**, *457*, 868.
[48] Z. Li, Z. Huang, F. Sun, X. Li, J. Ma, *Mater. Today Adv.* **2020**, *7*, 100077.
[49] X. Li, S. Xiao, X. Niu, J. S. Chen, Y. Yu, *Adv. Funct. Mater.* **2021**, *31*, 2104798.
[50] J. Cui, P. Ma, W. Li, R. Jiang, L. Zheng, Y. Lin, C. Guo, X. Yin, L. Wang, *Nano Res.* **2021**, *14*, 4714.
[51] W. Klement, R. Willens, P. Duwez, *Nature* **1960**, *187*, 869.
[52] W.-H. Wang, C. Dong, C. Shek, *Mater. Sci. Eng. R* **2004**, *44*, 45.
[53] W. L. Johnson, *MRS Bull.* **1999**, *24*, 42.
[54] A. L. Greer, *Science* **1995**, *267*, 1947.
[55] A. Inoue, A. Takeuchi, *Acta Mater.* **2011**, *59*, 2243.
[56] G. Duan, A. Wiest, M. L. Lind, J. Li, W. K. Rhim, W. L. Johnson, *Adv. Mater.* **2007**, *19*, 4272.
[57] B. Sarac, J. Eckert, *Prog. Mater. Sci.* **2022**, 100941.
[58] X. Li, D. Wei, J. Zhang, X. Liu, Z. Li, T. Wang, Q. He, Y. Wang, J. Ma, W. Wang, *Appl. Mater. Today* **2020**, *21*, 100866.
[59] J. Ma, X. Liang, X. Wu, Z. Liu, F. Gong, *Sci. Rep.* **2015**, *5*, 1.
[60] C. A. Schuh, T. C. Hufnagel, U. Ramamurty, *Acta Mater.* **2007**, *55*, 4067.
[61] M. M. Trexler, N. N. Thadhani, *Prog. Mater. Sci.* **2010**, *55*, 759.
[62] M. Ma, R. Liu, Y. Xiao, D. Lou, L. Liu, Q. Wang, W. Wang, *Mater. Sci. Eng., A* **2004**, *386*, 326.
[63] D. Wang, S. Wang, J. Wang, *Corros. Sci.* **2012**, *59*, 88.

[64] L. Zhang, L. Qiu, Q. Zhu, X. Liang, J. Huang, M. Yang, Z. Zhang, J. Ma, J. Shen, *Appl. Catal. B* **2021**, *294*, 120258.
[65] Y. C. Hu, Y. Z. Wang, R. Su, C. R. Cao, F. Li, C. W. Sun, Y. Yang, P. F. Guan, D. W. Ding, Z. L. Wang, *Adv. Mater.* **2016**, *28*, 10293.
[66] J. Ma, C. Yang, X. Liu, B. Shang, Q. He, F. Li, T. Wang, D. Wei, X. Liang, X. Wu, *Sci. Adv.* **2019**, *5*, eaax7256.
[67] H. Li, Z. Li, J. Yang, H. B. Ke, B. Sun, C. C. Yuan, J. Ma, J. Shen, W. H. Wang, *Sci. China Mater.* **2021**, *64*, 964.
[68] J. Fu, J. Yang, K. Wu, H. Lin, W. Wen, W. Ruan, S. Ren, Z. Zhang, X. Liang, J. Ma, *Mater. Horizon* **2021**, *8*, 1690.
[69] J. Ma, J. Yi, D. Zhao, M. Pan, W. Wang, *J. Appl. Phys.* **2012**, *112*, 064505.
[70] N. Li, W. Chen, L. Liu, *JOM* **2016**, *68*, 1246.
[71] G. Kumar, A. Desai, J. Schroers, *Adv. Mater.* **2011**, *23*, 461.
[72] J. Schroers, *Adv. Mater.* **2010**, *22*, 1566.
[73] J. Ma, X. Zhang, W. Wang, *J. Appl. Phys.* **2012**, *112*, 024506.
[74] R. Busch, J. Schroers, W. Wang, *MRS Bull.* **2007**, *32*, 620.
[75] R. Li, Z. Chen, A. Datye, G. H. Simon, J. Ketkaew, E. Kinser, Z. Liu, C. Zhou, O. E. Dagdeviren, S. Sohn, *Commun. Phys.* **2018**, *1*, 1.
[76] J. Ma, L. Huo, D. Zhao, W. Wang, *J. Appl. Phys.* **2013**, *113*, 104505.
[77] L. Liu, M. Hasan, G. Kumar, *Nanoscale* **2014**, *6*, 2027.
[78] Y. Yan, C. Wang, Z. Huang, J. Fu, Z. Lin, X. Zhang, J. Ma, J. Shen, *J. Mater. Chem. A* **2021**, *9*, 5415.
[79] J. Schroers, *JOM* **2005**, *57*, 35.
[80] H. M. Chiu, G. Kumar, J. Blawzdziewicz, J. Schroers, *Scr. Mater.* **2009**, *61*, 28.
[81] X. Liu, Y. Shao, J.-F. Li, N. Chen, K.-F. Yao, *J. Alloys Compd.* **2014**, *605*, 7.
[82] Z. Liu, J. Schroers, *Nanotechnology* **2015**, *26*, 145301.
[83] J. Fu, Z. Huang, J. Yang, J. Ma, J. Shen, *J. Non-Cryst. Solids* **2021**, *558*, 120682.
[84] P. Gong, S. Wang, Z. Liu, W. Chen, N. Li, X. Wang, K. Yao, *Intermetallics* **2018**, *98*, 54.
[85] J. Chu, H. Wijaya, C. Wu, T.-R. Tsai, C. Wei, T. Nieh, J. Wadsworth, *Appl. Phys. Lett.* **2007**, *90*, 034101.
[86] X. Liu, N. Chen, J.-L. Gu, G.-N. Yang, G. Mussler, K.-F. Yao, *Mater. Des.* **2015**, *87*, 1018.
[87] K. Takenaka, N. Togashi, N. Nishiyama, A. Inoue, *J. Non-Cryst. Solids* **2010**, *356*, 1542.
[88] R. C. Sekol, G. Kumar, M. Carmo, F. Gittleson, N. Hardesty-Dyck, S. Mukherjee, J. Schroers, A. D. Taylor, *Small* **2013**, *9*, 2081.
[89] M. Hasan, J. Schroers, G. Kumar, *Nano Lett.* **2015**, *15*, 963.
[90] J. Ma, X. Zhang, D. Wang, D. Zhao, D. Ding, K. Liu, W. Wang, *Appl. Phys. Lett.* **2014**, *104*, 173701.
[91] G. Kumar, P. A. Staffier, J. Blawzdziewicz, U. D. Schwarz, J. Schroers, *Appl. Phys. Lett.* **2010**, *97*, 101907.
[92] C. Zhou, A. Datye, Z. Chen, G. H. Simon, X. Wang, J. Schroers, U. D. Schwarz, *APL Mater.* **2020**, *8*, 111104.
[93] Y. Wu, D. Cao, Y. Yao, G. Zhang, J. Wang, L. Liu, F. Li, H. Fan, X. Liu, H. Wang, *Nat. Commun.* **2021**, *12*, 1.
[94] M. Shi, Z. Liu, T. Zhang, *J. Mater. Sci. Technol.* **2015**, *31*, 493.
[95] J. Zhu, W. Gao, S. Cheng, X. Liu, X. Yang, J. Tian, J. Ma, J. Shen, *J. Alloys Compd.* **2022**, 164679.
[96] J. Yu, Y. Ding, C. Xu, A. Inoue, T. Sakurai, M. Chen, *Chem. Mater.* **2008**, *20*, 4548.
[97] L. Y. Chen, J. S. Yu, T. Fujita, M. W. Chen, *Adv. Funct. Mater.* **2009**, *19*, 1221.
[98] Z. Jia, K. Nomoto, Q. Wang, C. Kong, L. Sun, L. C. Zhang, S. X. Liang, J. Lu, J. J. Kruzic, *Adv. Funct. Mater.* **2021**, *31*, 2101586.
[99] G. Doubek, R. C. Sekol, J. Li, W. H. Ryu, F. S. Gittleson, S. Nejati, E. Moy, C. Reid, M. Carmo, M. Linardi, *Adv. Mater.* **2016**, *28*, 1940.
[100] Y. Xu, J. Cheng, P. M. Yiu, G. Shan, T. Shibayama, S. Watanabe, M. Ohnuma, C.-H. Shek, *Nanoscale* **2018**, *10*, 18846.
[101] M.-X. Li, S.-F. Zhao, Z. Lu, A. Hirata, P. Wen, H.-Y. Bai, M. Chen, J. Schroers, Y. Liu, W.-H. Wang, *Nature* **2019**, *569*, 99.
[102] D. Liu, Z. Song, S. Cheng, Y. Wang, A. Saad, S. Deng, J. Shen, X. Huang, X. Cai, P. Tsiakaras, *Chem. Eng. J.* **2022**, *431*, 134210.
[103] H. Qian, X. Mu, K. Li, S. Xie, X. Xiong, X. Zeng, *Mater. Sci. Technol.* **2020**, *36*, 1083.
[104] J. Song, F. Zhang, Q. Hu, D. Lu, Z. Lu, B. Zhang, *Appl. Surf. Sci.* **2022**, 153123.
[105] R. Li, X. Liu, R. Wu, J. Wang, Z. Li, K. Chan, H. Wang, Y. Wu, Z. Lu, *Adv. Mater.* **2019**, *31*, 1904989.
[106] S. Ju, J. Feng, P. Zou, W. Xu, S. Wang, W. Gao, H.-J. Qiu, J. Huo, J.-Q. Wang, *J. Mater. Chem. A* **2020**, *8*, 3246.
[107] C. Wang, Z. Li, S. Zhu, Y. Liang, Z. Cui, S. Wu, C. Qin, S. Luo, A. Inoue, *Sci. China Mater.* **2021**, *64*, 2289.
[108] Y.-Y. Zhao, F. Qian, C. Zhao, C. Xie, J. Wang, C. Chang, Y. Li, L.-C. Zhang, *J. Mater. Sci. Technol.* **2021**, *70*, 205.
[109] J. Zeleny, *Phys. Rev.* **1914**, *3*, 69.
[110] J.-W. Jung, W.-H. Ryu, J. Shin, K. Park, I.-D. Kim, *ACS Nano* **2015**, *9*, 6717.
[111] K. S. Nakayama, Y. Yokoyama, T. Wada, N. Chen, A. Inoue, *Nano Lett.* **2012**, *12*, 2404.
[112] W. Jiao, P. Liu, H. Lin, W. Zhou, Z. Wang, T. Fujita, A. Hirata, H.-W. Li, M. Chen, *Chem. Mater.* **2017**, *29*, 4478.
[113] Y. Liu, J. Liu, S. Sohn, Y. Li, J. J. Cha, J. Schroers, *Nat. Commun.* **2015**, *6*, 1.
[114] M. Zhao, K. Abe, S.-I. Yamaura, Y. Yamamoto, N. Asao, *Chem. Mater.* **2014**, *26*, 1056.
[115] J. Johny, Y. Li, M. Kamp, O. Prymak, S.-X. Liang, T. Krekeler, M. Ritter, L. Kienle, C. Rehbock, S. Barcikowski, *Nano Res.* **2022**, *15*, 4807.
[116] S.-X. Liang, S. Salamon, S. Zerebecki, L.-C. Zhang, Z. Jia, H. Wende, S. Reichenberger, S. Barcikowski, *Scr. Mater.* **2021**, *203*, 114094.
[117] W. Yan, I. Richard, G. Kurtuldu, N. D. James, G. Schiavone, J. W. Squair, T. Nguyen-Dang, T. Das Gupta, Y. Qu, J. D. Cao, *Nat. Nanotechnol.* **2020**, *15*, 875.
[118] Y. He, Y. Peng, Z. Li, J. Ma, X. Zhang, K. Liu, W. Wang, L. Jiang, *Sci. China Chem.* **2016**, *59*, 271.
[119] Q. Jiang, Y. Wang, Y. Xie, M. Zhou, Q. Gu, Z. Zhong, W. Xing, *Water Res.* **2022**, *216*, 118270.
[120] J. Wang, H. Wang, J. Xie, A. Yang, A. Pei, C.-L. Wu, F. Shi, Y. Liu, D. Lin, Y. Gong, *Energy Storage Mater.* **2018**, *14*, 345.
[121] H. Jiang, J. Li, C. Cao, X. Liu, M. Liu, Y. Shen, Y. Liu, Q. Zhang, W. Wang, L. Gu, *Nano Res.* **2019**, *12*, 2808.
[122] H. Xian, M. Liu, X. Wang, F. Ye, P. Wen, H. Bai, Y. Liu, W. Wang, *Nanotechnology* **2018**, *30*, 085705.
[123] W.-T. Chen, K. Manivannan, C.-C. Yu, J. P. Chu, J.-K. Chen, *Nanoscale* **2018**, *10*, 1366.
[124] R. C. Sekol, M. Carmo, G. Kumar, F. Gittleson, G. Doubek, K. Sun, J. Schroers, A. D. Taylor, *Int. J. Hydrogen Energy* **2013**, *38*, 11248.
[125] X. Liu, S. Ju, P. Zou, L. Song, W. Xu, J. Huo, J. Yi, G. Wang, J.-Q. Wang, *J. Alloys Compd.* **2021**, *880*, 160548.
[126] Z. Jia, Y. Zhao, Q. Wang, F. Lyu, X. Tian, S.-X. Liang, L.-C. Zhang, J. Luan, Q. Wang, L. Sun, *ACS Appl. Mater. Interfaces* **2022**, *14*, 10288.
[127] M. Carmo, R. C. Sekol, S. Ding, G. Kumar, J. Schroers, A. D. Taylor, *ACS Nano* **2011**, *5*, 2979.
[128] L.-C. Zhang, Z. Jia, F. Lyu, S.-X. Liang, J. Lu, *Prog. Mater. Sci.* **2019**, *105*, 100576.
[129] S. X. Liang, Z. Jia, Y. J. Liu, W. Zhang, W. Wang, J. Lu, L. C. Zhang, *Adv. Mater.* **2018**, *30*, 1802764.
[130] Z. Jia, J. Kang, W. Zhang, W. Wang, C. Yang, H. Sun, D. Habibi, L. Zhang, *Appl. Catal., B* **2017**, *204*, 537.

[131] S. Chen, M. Li, Q. Ji, T. Feng, S. Lan, K. Yao, *J. Mater. Sci. Technol.* **2022**, *117*, 49.
[132] Z. Li, X. Qin, Z. Zhu, S. Zheng, H. Li, H. Fu, H. Zhang, *J. Mater. Chem. A* **2020**, *8*, 10855.
[133] X. Qin, J. Xu, Z. Zhu, Z. Li, D. Fang, H. Fu, S. Zhang, H. Zhang, *J. Mater. Sci. Technol.* **2022**, *113*, 105.
[134] Z. Jia, J.-L. Jiang, L. Sun, L.-C. Zhang, Q. Wang, S.-X. Liang, P. Qin, D.-F. Li, J. Lu, J. J. Kruzic, *ACS Appl. Mater. Interfaces* **2020**, *12*, 44789.
[135] S.-X. Liang, X. Wang, W. Zhang, Y.-J. Liu, W. Wang, L.-C. Zhang, *Appl. Mater. Today* **2020**, *19*, 100543.
[136] Z. Jia, Q. Wang, L. Sun, Q. Wang, L. C. Zhang, G. Wu, J. H. Luan, Z. B. Jiao, A. Wang, S. X. Liang, *Adv. Funct. Mater.* **2019**, *29*, 1807857.
[137] C. Yang, C. Zhang, W. Xing, L. Liu, *Intermetallics* **2018**, *94*, 22.
[138] Z. Li, S. Feng, Y. Liu, J. Hu, C. Wang, B. Wei, *Adv. Opt. Mater.* **2019**, *7*, 1900845.
[139] M. Li, M. Shi, B. Wang, C. Zhang, S. Yang, Y. Yang, N. Zhou, X. Guo, D. Chen, S. Li, *Adv. Funct. Mater.* **2021**, *31*, 2102840.
[140] J. Padmanabhan, E. R. Kinser, M. A. Stalter, C. Duncan-Lewis, J. L. Balestrini, A. J. Sawyer, J. Schroers, T. R. Kyriakides, *ACS Nano* **2014**, *8*, 4366.
[141] J. Wang, A. M. Loye, J. Ketkaew, J. Schroers, T. R. Kyriakides, *ACS Appl. Bio Mater.* **2018**, *1*, 51.
[142] J. Padmanabhan, M. J. Augelli, B. Cheung, E. R. Kinser, B. Cleary, P. Kumar, R. Wang, A. J. Sawyer, R. Li, U. D. Schwarz, *Sci. Rep.* **2016**, *6*, 1.
[143] M. Shayan, J. Padmanabhan, A. H. Morris, B. Cheung, R. Smith, J. Schroers, T. R. Kyriakides, *Acta Biomater.* **2018**, *75*, 427.
[144] A. M. Loye, E. R. Kinser, S. Bensouda, M. Shayan, R. Davis, R. Wang, Z. Chen, U. D. Schwarz, J. Schroers, T. R. Kyriakides, *Sci. Rep.* **2018**, *8*, 1.
[145] F. Sun, B. Wang, F. Luo, Y. Q. Yan, H. B. Ke, J. Ma, J. Shen, W. H. Wang, *Mater. Des.* **2020**, *190*, 108595.
[146] T. Zou, B. Zhao, W. Xin, Y. Wang, B. Wang, X. Zheng, H. Xie, Z. Zhang, J. Yang, C. Guo, *Light Sci. Appl.* **2020**, *9*, 1.
[147] Y. Tian, X. Liu, A. Caratenuto, J. Li, S. Zhou, R. Ran, F. Chen, Z. Wang, K.-T. Wan, G. Xiao, *Nano Energy* **2022**, *92*, 106717.
[148] B. Jiang, X. Jia, T. Ji, M. Zhou, J. He, K. Wang, J. Tian, X. Yan, K. Fan, *Sci. China Life Sci.* **2022**, *65*, 328.
[149] Q. Lei, D. He, L. Ding, F. Kong, P. He, J. Huang, J. Guo, C. J. Brinker, G. Luo, W. Zhu, *Adv. Funct. Mater.* **2022**, 2113269.
[150] X. Fan, Y. Yang, X. Shi, Y. Liu, H. Li, J. Liang, Y. Chen, *Adv. Funct. Mater.* **2020**, *30*, 2007110.
[151] X. Liang, Y. Liu, Z. Liu, J. Ma, Z. Zhang, W. Ruan, S. Ren, T. Peng, X. Wu, H. Shi, *Mater. Des.* **2021**, *205*, 109771.
[152] Y. Zhou, L. Jiang, *Joule* **2020**, *4*, 2244.
[153] M. Wang, P. Zeng, S. Bai, J. Gu, F. Li, Z. Yang, M. Liu, *Sol. RRL* **2018**, *2*, 1800217.
[154] J. D. Benck, T. R. Hellstern, J. Kibsgaard, P. Chakthranont, T. F. Jaramillo, *ACS Catal.* **2014**, *4*, 3957.
[155] X. Song, K. Xiao, X. Wu, G. Wilde, M. Jiang, *J. Non-Cryst. Solids* **2019**, *517*, 119.
[156] M. Hasan, G. Kumar, *Nanoscale* **2017**, *9*, 3261.
[157] V. Hasannaeimi, X. Wang, R. Salloom, Z. Xia, J. Schroers, S. Mukherjee, *ACS Appl. Energy Mater.* **2020**, *3*, 12099.
[158] Z. Huang, J. Fu, X. Li, W. Wen, H. Lin, Y. Lou, F. Luo, Z. Zhang, X. Liang, J. Ma, *Sci. China Mater.* **2022**, *65*, 255.
[159] S. Mukherjee, M. Carmo, G. Kumar, R. C. Sekol, A. D. Taylor, J. Schroers, *Electrochim. Acta* **2012**, *74*, 145.
[160] Y. Chen, J. Chu, J. Jang, C. Wu, *Mater. Sci. Eng. A* **2012**, *556*, 488.
[161] X. Liu, Y. Shao, Y. Tang, K.-F. Yao, *Sci. Rep.* **2014**, *4*, 1.
[162] N. Li, T. Xia, L. Heng, L. Liu, *Appl. Phys. Lett.* **2013**, *102*, 251603.
[163] E. R. Kinser, J. Padmanabhan, R. Yu, S. L. Corona, J. Li, S. Vaddiraju, A. Legassey, A. Loye, J. Balestrini, D. A. Solly, *ACS Sens.* **2017**, *2*, 1779.
[164] W. Zhang, H. Miao, Y. Li, C. Chang, G. Xie, X. Jia, *J. Alloys Compd.* **2017**, *707*, 57.
[165] J. Kobata, K.-I. Miura, K. Amiya, Y. Fukuda, Y. Saotome, *J. Alloys Compd.* **2017**, *707*, 132.
[166] P. Gong, H. Kou, S. Wang, L. Deng, X. Wang, J. Jin, *J. Alloys Compd.* **2019**, *801*, 267.
[167] Z. Hu, C. Uzun, Z. Dong, W. Li, A. A. Bernussi, G. Kumar, *Appl. Phys. Lett.* **2017**, *111*, 023107.
[168] S. Cheng, J. Ma, F. Gong, J. Shen, *Metals* **2021**, *11*, 1520.
[169] H. Wang, R. Wei, X. Li, X. Ma, X. Hao, G. Guan, *J. Mater. Sci. Technol.* **2021**, *68*, 191.
[170] S. Jiang, L. Zhu, Z. Yang, Y. Wang, *Int. J. Hydrogen Energy* **2021**, *46*, 36731.
[171] F. Li, S. Wang, L. Gu, X. Chang, H. Lin, K. Wu, *Ionics* **2022**, *28*, 1367.
[172] K. Aneeshkumar, J.-C. Tseng, X. Liu, J. Tian, D. Diao, J. Shen, *RSC Adv.* **2021**, *11*, 7369.
[173] C. Pei, S. Chen, T. Zhao, M. Li, Z. Cui, B. Sun, S. Hu, S. Lan, H. Hahn, T. Feng, *Adv. Mater.* **2022**, 2200850.
[174] Y. Jin, G. Xi, R. Li, Z.-A. Li, X.-B. Chen, T. Zhang, *J. Alloys Compd.* **2021**, *852*, 156876.
[175] M. T. Kiani, C. M. Barr, S. Xu, D. Doan, Z. Wang, A. Parakh, K. Hattar, X. W. Gu, *Nano Lett.* **2020**, *20*, 6481.

Jianan Fu received the B.S. degree from Jiangxi Agricultural University in 2019 and the master degree in mechanical engineering from Shenzhen University in 2022. He will study for a PhD at Southern University of science and technology. His research includes micro/nano-structure by the thermoplastic forming process and functional application of metallic glasses.

Jiang Ma received the B.S. degree in materials science and engineering from Southeast University in 2009 and the Ph.D. degree from the Institute of Physics, Chinese Academy of Sciences (CAS), Beijing, China, in 2014, and received the Outstanding PhD student Award (Top 1%) and Institute Director Honored Award (Top 5%). He is currently a Professor in the College of Mechatronics and Control Engineering, Shenzhen University, China, and received the Outstanding Teacher Award of Shenzhen, 2018. His research includes the forming, functional application and high frequency dynamic loading behavior of metallic glasses.

